**Title:** Eukaryotic influence on the oceanic biological carbon pump in the Scotia Sea as revealed by 18S rRNA gene sequencing of suspended and sinking particles

**Authors:** Manon T Duret[1]*, Richard S Lampitt[2], Phyllis Lam[1]

[1]Ocean and Earth Science, University of Southampton

[2]National Oceanography Centre Southampton

*Corresponding author:

Manon Duret,

Ocean and Earth Science, University of Southampton,

National Oceanography Centre Southampton

European Way, Southampton, SO14 3ZH,

United Kingdom

Tel: +44 (0)23 8059 2786

Email: M.T.Duret@soton.ac.uk

**Running head:** Eukaryotic influence on marine particles

**Keywords:** Eukaryotic phytoplankton; 18S rRNA gene sequencing; marine particles; suspended versus sinking; biological carbon pump.

**Abstract**

Suspended marine particles constitute most of the particulate organic matter pool in the oceans thereby providing substantial substrates for heterotrophs, especially in the mesopelagic. Conversely, sinking particles are major contributors to carbon fluxes defining the strength of the biological carbon pump (BCP). This study is the first to investigate the differential influence of eukaryotic communities to suspended and sinking particles, using 18S rRNA gene sequencing on particles collected with a marine snow catcher in the mixed layer and upper-mesopelagic of the Scotia Sea, Southern Ocean. In the upper-mesopelagic, most eukaryotic phytoplankton sequences belonged to chain-forming diatoms in sinking particles and to prymnesiophytes in suspended particles. This suggests that diatom-enriched particles are more efficient in carbon transfer to the upper-mesopelagic than those enriched in prymnesiophytes in the Scotia Sea, the latter more easily disintegrating into suspended particles. In the upper-mesopelagic, copepods appeared most influential on sinking particles whereas soft-tissue metazoan sequences contributed more to suspended particles. Heterotrophic protists and fungi communities were distinct between mixed layer and upper mesopelagic, implying that few protists ride along on sinking particles. Furthermore, differences between predatory flagellates and radiolarians between suspended and sinking particles implied different ecological conditions between the two particles pools, and roles in the BCP. Molecular analyses of sinking and suspended particles constitute powerful diagnostic tools to study the eukaryotic influence on the BCP in a more holistic manner compared to classic carbon export studies focusing on sinking particles.

## Introduction

The oceanic biological carbon pump (BCP) corresponds to the processes by which organic matter produced by phytoplankton's photosynthesis in the sunlit epipelagic ocean (upper ~100 m) is exported to depth, thereby sequestrating atmospheric carbon in the mesopelagic (~ 100 to 1000 m) and deeper ocean (Turner 2015). This downward export of organic matter removes each year more than 10 billion tons of carbon from the epipelagic (Buesseler and Boyd 2009), representing 5 to 25 % of the euphotic photosynthetic primary production reaching the mesopelagic (De La Rocha and Passow 2007). Most of this autochthonous carbon flux occurs in the form of particulate organic matter (POM). POM consists of a combination of different materials such as faecal pellets, living and non-living microbial cells and fragments of cells, empty larvacean houses – all of which, if occurring on their own, can be incorporated into large aggregated entities known as marine snow. In coastal systems some allochthonous POM, such as from river run-offs, can also constitute sinking particles. The nature of these sinking particles depends largely on the structure of phytoplankton community (Korb et al. 2012) and heterotrophic community members, including mesozooplankton (> 200 µm) (Steinberg and Landry 2017) and heterotrophic microbes (prokaryotes and unicellular eukaryotes or protists) (Worden et al. 2015).

Heterotrophic communities alter the BCP efficiency, either *(i)* negatively by reducing carbon export owing to remineralisation processes that release carbon dioxide ($CO_2$) and inorganic nutrients (Cho and Azam 1988; Smith et al. 1992; Kiørboe and Jackson 2001; Steinberg et al. 2008; Collins et al. 2015); or *(ii)* positively by enhancing carbon export to depth. Mesozooplankton can indeed lead to an increase of particle export by grazing on phytoplankton cells and other small particles, and subsequently repackaging them into larger faecal pellets (≥ 50 µm depending on the species) (Stamieszkin et al. 2017) which can sink then faster to depth (Atkinson et al. 2001; Giesecke et al. 2010; Ebersbach et al. 2011), although not all faecal pellets sink (Lampitt et al. 1990). Additionally, vertical migration of mesozooplankton may lead to the active transfer of organic matter from one depth to another, as they feed on POM in the epipelagic and release faecal pellets and dissolved organic matter (DOM) at greater depths (Steinberg et al. 2000). Examples include decapods (Pakhomov *et al.*, 2018), copepods (Cavan *et al.*, 2015; Yebra *et al.*, 2018) and gelatinous zooplankton (Alldredge, 1976; Wilson *et al.*, 2008). Conversely, they can release DOM and break sinking particles into smaller pieces that remain in suspension in the water column (suspended particles) (De La Rocha and Passow 2007) via sloppy feeding (Strom et al. 1997). The proportion of suspended particles originating from the disaggregation of sinking particles is currently unknown (Lam and Marchal 2015), as it is governed by complex abiotic and biotic processes such as those mentioned above, as well as feeding behaviours of micro- and nanozooplankton (protists 20–200 µm and 2–20 µm, respectively) (Ploug and Grossart 2000; Poulsen and Iversen 2008).

Heterotrophic protists, such as flagellates and ciliates, are enriched in large sinking particles relative to surrounding waters (Simon et al. 2002), even in the bathypelagic ocean (~1000-4000 m) (Bochdansky et al. 2017). Micro- and nanozooplankton consume ~60 % of the daily phytoplankton primary production (Calbet and Landry 2004; Schmoker et al. 2013). By doing so, they can contribute to carbon export by producing “minipellets” (3–50 µm faecal pellets) when dense enough (Gowing and Silver 1985). However, they also allow organic matter to enter the microbial loop, thereby lengthening the “food chain” while reducing carbon export (Pomeroy and Wiebe 1988; Legendre and Le Fevre 1995; Legendre and Rassoulzadegan 1996). Although studies have focused on differences between various sizes of freely suspended and particle-associated protists – e.g., cut-off sizes at 30 µm (Duret et al. 2015; Bochdansky et al. 2017) and 1.6 µm (Parris et al. 2014), these communities remain largely understudied (Edgcomb 2016; Caron 2017). Similarly, fungal communities in open-ocean and polar systems remain poorly known (Grossart et al. 2019), although studies have shown their importance in the degradation of marine snow (Bochdansky et al. 2017).

While heterotrophs lead to a decrease of sinking particles concentration of with depth (Martin et al. 1987; Francois et al. 2002), the quantity of suspended particles remains constant with depth, with their organic carbon content generally at two or more orders of magnitude higher than that of sinking particles (Bishop et al. 1977; Bacon et al. 1985; Verdugo et al. 2004; Riley et al. 2012; Giering et al. 2014; Baker et al. 2017; Cavan et al. 2017). Especially in the mesopelagic, suspended particles constitute major organic carbon substrates for heterotrophs, including microbes (Baltar et al. 2009, 2010; Herndl and Reinthaler 2013) and micronekton (e.g., fish, cephalopods and crustaceans) (Gloeckler et al. 2017). Like sinking particles, they are hotspots for microbial activity (Bochdansky et al. 2010) and diversity (Duret et al. 2018). However, most studies on particle-associated microbial communities so far have focused on sinking particles, and primarily on prokaryotes (e.g., Delong et al. 1993; López-Pérez et al. 2012; Crespo et al. 2013; Mestre et al. 2017).

The main reason behind this knowledge gap is owed to the fact that conventional sampling methodologies used for marine microbial communities are unable to distinguish between suspended and sinking particles. They either collect a mixture of both particle pools in unknown proportions (e.g, size-fractionated filtration of seawater), or mainly large sinking particles (e.g., sediment traps) (McDonnell et al. 2015). The marine snow catcher (MSC) (Lampitt et al. 1993) is a large water-sampler that uses sinking velocity to differentiate suspended from sinking particles originating from the same water sample. This is the first study to investigate the differential contribution of eukaryotic communities in sinking and suspended particles collected with an MSC using 18S rRNA gene amplicon sequencing –

either as direct residents within particles or as fragments of dead organisms (including phytoplankton, metazoans and heterotrophic protists).

18S rRNA gene amplicon sequencing has been used to investigate eukaryotic plankton taxonomic communities distribution and their inferred preferential ecological niches at large scales (e.g., Pernice et al. 2013, 2015; de Vargas et al. 2015), as well as in specific oceanic environments (e.g., Sauvadet et al. 2010; Orsi et al. 2012). Comparing the taxonomic composition of eukaryotic communities associated with sinking particles from the mixed layer with sinking particles from the upper-mesopelagic would help assessing the continuity of particle composition with depth, and thus identifying key contributors to carbon export. Furthermore, comparing the taxonomic composition of sinking particles from the mixed layer with suspended particles in the upper-mesopelagic would inform us on particle dynamics and the influence of sinking particle disaggregation on suspended particle composition (Lam and Marchal 2015). More specifically, our objectives were to assess *(i)* which eukaryotic phytoplankton taxa are the most efficient in particulate carbon export to the mesopelagic in the Scotia Sea, *(ii)* what metazoan and eukaryotic phytoplankton taxa contribute to sinking and suspended particles in the upper-mesopelagic, and *(iii)* if the heterotrophic protist compositions in the two particle pools differ in the mesopelagic, such that they have different roles in particle attenuation and the BCP.

## Materials

### *Study site*

Sampling took place during the austral summer 2014 (15 November – 12 December) on-board the *RRS James Clark Ross* (cruise JR304). In the Scotia Sea, four stations of contrasting nutrient regimes and surface productivity were sampled, including two low-productivity stations – ICE (59.9624˚S, 46.1597˚W) and P2 (55.2484˚S, 41.2640˚W) – and two additional higher productive stations – P3 (52.8121˚S, 39.9724˚W) and UP (52.06018˚S, 39.1994˚W). Surface particulate organic carbon data is presented on a map constructed with the Ocean Data View software (https://odv.awi.de) using the mean values for December 2014 deduced from ocean colour by the MODIS satellite (http://oceancolor.gsfc.nasa.gov/cgi/l3) (Fig. 1).

Temperature, oxygen concentration and chlorophyll *a* concentration based on fluorescence measurements were measured with a conductivity-temperature-depth device (CTD Seabird 9Plus with SBE32 carousel) (Fig. S1). Particulate organic carbon (POC) concentrations were measured by and are presented in Belcher et al. (2016) from samples collected with an marine snow catcher (MSC) on the same cruise.

### *Particle sampling*

Particles were collected with an MSC deployed at the base of the mixed layer and in the upper-mesopelagic (~110 m below the deep chlorophyll maximum). Both deployments occurred within ~30 minutes of each other. The former depth was chosen because it usually corresponds to a peak in particle abundance in this region (Belcher et al., 2016). The latter depth was chosen as it is usually the region where the sharpest decline in particle concentration with depth is observed, and where transfer efficiency of the BCP is usually determined (Buesseler and Boyd 2009). These depths were defined using fluorescence profiles taken during CTD cast deployed maximum 4 hours prior to MSC deployments (Fig. S1).

After its retrieval from the desired depth, the MSC is left undisturbed on the ship's deck for two hours. This period allows sinking particles to settle at the bottom of the sampler (MSCB) while suspended particles remain in suspension in the upper part (MSCU), as described and illustrated in Riley et al. (2012) and Duret et al. (2018). Water samples are collected from the

MSCU followed by the MSCB. Sinking particles are defined here as the particles that have sunk to the MSCB after 2 hours (average sinking velocity $\geq 12$ m $d^{-1}$) and include both slow- and fast-sinking particles (Riley et al. 2012). Particles remaining in suspension in the MSCU are considered suspended. Both sinking and suspended particles consisted of a mixture of single free-living cells and cells associated with particles or aggregates. Each MSCU sample was subsequently size-fractionated to further separate collected particles into size-classes.

Suspended particles were sampled by sequentially filtering ~10 L of seawater collected from the MSCU through; *(i)* a 100 µm pore-size nylon filter (47 mm diameter, Millipore), *(ii)* a 10 µm pore-size polycarbonate membrane filter (47 mm diameter, Millipore), and *(iii)* a 0.22 µm pore-size Sterivex cartridge filter (Millipore) driven by a peristaltic pump. Sinking particles were collected by gravity-filtering ~1.5 L of seawater collected from the MSCB onto a 10 µm pore-size polycarbonate membrane filter. Both filtering steps were performed in under 1 hour, and filters were subsequently incubated with RNAlater (Ambion™, Thermo Fisher Scientific) for 12 hours at 4˚C, prior to being stored at -80˚C until further processing onshore. In total, four particle-fractions were collected at each station and at each depth: *(i)* suspended particles 0.22–10 µm (referred to as SS0.22), *(ii)* 10–100 µm (SS10), *(iii)* ≥ 100 µm (SS100), and *(iv)* sinking particles ≥ 10 µm (SK10).

### ***DNA extraction and sequencing***

Nucleic acids were recovered from the filters using a ToTALLY RNA kit (Ambion™, Thermo Fisher Scientific) followed by a DNA extraction step as described in Lam *et al.* (2011) – though only DNA extracts were considered in this study. Extracted DNA was further purified with a Wizard DNA clean-up system (Promega) following manufacturer's recommendations.

Amplicon sequencing of eukaryotic 18S rDNA V4 region was performed according to Hadziavdic *et al.* (2014) and following the Illumina "16S metagenomic sequencing library preparation" protocol. The primer set F-574 (5'-GCGGTAATTCCAGCTCCAA-3') and R-952 (5'-TTGGCAAATGCTTTCGC-3'; 378 bp), including overhang adapters (respectively 5'-TCGTCGGCAGCGTCAGATGTGTATAAGAGACAG-3' and 5'-GTCTCGTGGGCTCGGAGATGTGTATAAGAGACAG-3'), was used for the first PCR, with each reaction comprising 2.5 µL of purified DNA extract, 5 µL of each forward and reverse primers, 12.5 µL of 2X proofreading polymerase Kapa Hifi Hotstart ready mix (Kapa Biosystems). The PCR conditions followed were: 95˚C for 3 min, 25 cycles of 95˚C for 30 sec, 55˚C for 30 sec and 72˚C for 30 sec, and finally 72˚C for 5 min. These amplicons were subsequently used as templates for an indexing PCR for the overhangs to be linked to Illumina sequencing adapters and indices (Nextera XT Index Primer 1, i7, and Primer 2, i5) for downstream sequencing. Each PCR reaction included 5 µL of amplicon from the first PCR, 5 µL of each Nextera primers and 10 µL of PCR-grade water, 25 µL 2X Kapa Hifi Hotstart ready mix, and followed PCR conditions of 95˚C for 3 min, 10 cycles of 95˚C for 30 sec, 55˚C for 30 sec and 72˚C for 30 sec, and a final extension at 72˚C for 5 min. For the samples showing a total amount of extracted DNA less than 12.5 ng (ICE SS10 mixed layer, UP and P3 SS100 upper-mesopelagic), a nested PCR approach was applied including an additional amplification with the universal 18S rDNA primers set prior to the two-step PCR described above. This procedure caused little variation in the OTU composition and structure of microbial communities, as evidenced in Duret et al. (2018). After each PCR round, amplicons were purified with the Agencourt AMPure XP PCR clean-up kit (Beckman Coulter) following manufacturer's recommendations. The quality of purified amplicons was assessed with a DNA7500 Kit read on a 2100 Bioanalyser (Agilent Technologies) and the quantity measured with a Qubit dsDNA High-Sensitivity assay kit (Invitrogen™, Thermo

Fisher Scientific). Purified amplicons were pooled at equimolar concentrations (4 nM each) for the library preparation using a Nextera XT DNA kit (Illumina) following manufacturer's recommendations and included 5 % PhiX. Finally, the amplicons were sequenced with an Illumina MiSeq sequencing system (M02946, Illumina) using a MiSeq Reagent 600-cycle Kit v3 (Illumina).

***Bioinformatics***

Raw sequences were demultiplexed and their adapters trimmed using the MiSeq Control software (v2.5.0.5, Ilumina) directly after sequencing. The quality of demultiplexed raw read pairs was checked with FastQC (v 0.11.4; Babraham Bioinformatics). Forward and reverse reads were merged with the PANDAseq assembler software (v 2.8) (Masella et al. 2012) using the default parameters (simple Bayesian algorithm for assembly), and a maximum read length of 500 bp and Phred33 quality score of 0.8. OTU clustering was subsequently performed under QIIME (MacQIIME v 1.9.1_20150604) (Caporaso et al. 2010) after all libraries were compiled into a single FASTA file using the *multiple_split_libraries_fastq.py* function. Clustering was performed using the open reference function *pick_open_reference_otus.py* using default parameters (UCLUST algorithm for OTU picking) using a minimum sequence identity of 97% against the SSU Silva database (v 128) (Quast et al. 2013), and against the $PR^2$ database (v 4.11.1) (Guillou et al. 2012) for heterotrophic protists and fungi. Singleton OTUs were discarded.

Based on taxonomic affiliation and/or physiological information, OTUs were divided into several categories for individual analyses and further discussions: phytoplankton, metazoans, dinoflagellates, choanoflagellates, *Syndiniales*, ciliates, rhizarians and fungi. This classification would have inadvertently included some ambiguities, such as the classification of certain mixotrophs/heterotrophs in the phytoplankton category (e.g., heterotrophic

*Stramenopiles*). Because high-throughput amplicon sequencing of the 18S rRNA gene is subject to PCR biases, it is important to note that relative abundances do not represent absolute quantities. Organisms with high gene copy numbers and DNA contents per cell would disproportionally be favoured (Zhu et al. 2005), leading to overrepresentation of these taxa (Medinger et al. 2010). Nonetheless, it is informative to compare relative abundances of specific taxa presenting similar copy numbers of the 18S rRNA gene (Gong et al. 2013), which was the primary purpose of the analyses presented in this study.

***Statistical analyses***

The canonical correspondence analysis (CCA) and permutational multivariate analyses of variance (PERMANOVA) were performed on the rarefied dataset and were used to investigate the significance of environmental and inherent sampling factors responsible for composition variability. The similarity percent analysis (SIMPER) was based on the Bray-Curtis dissimilarity distance of OTU composition and were used to investigate the differences between communities associated with different particle-fractions.

Taxa enrichments in the upper mesopelagic relative to sinking particles (SK10) in the mixed layer were calculated according to the following equation (1):

$$Enrichment = \log_2\left(\frac{RA_{sample\ UM}}{RA_{SK10\ ML}}\right) \qquad (1)$$

where $RA_{SK10\ ML}$ is the relative abundance of the taxa in SK10 mixed layer and $RA_{sample\ UM}$ is the relative abundance of the same taxa in the compared sample in the upper-mesopelagic. Therefore, negative values indicate an enrichment within mixed layer SK10 while positive values indicate an enrichment within the compared sample.

Analyses were performed with the R statistics software (http://www.r-project.org), using features of the *vegan* package. Statistical analyses were performed on the dataset rarefied to the smallest library size, either at a considered station and depth or overall (as would be indicated). For the calculation of SIMPER and the proportions of shared/unique OTUs, the dataset was rarefied to the smallest library size in a considered station (n = 16,127 sequences for ICE; 29,119 for P2; 6,055 for P3 and 28,937 for UP). Multivariate analyses comparing samples from all stations (CCA and PERMANOVA) were performed on the dataset rarefied to the smallest library size (n = 3,976 sequences/library).

## Results and Discussion

### *Sequencing statistics*

A total of 2,517,165 V4 18S rDNA paired-ends reads were recovered from all four particle-fractions (suspended particles 0.22– 0 µm [SS0.22], 10–100 µm [SS10], and ≥100 µm [SS100], as well as sinking particles ≥10 µm [SK10]). After sequence trimming, pairing and merging, and separation from metazoan sequences, a total of 1,533,266 protist sequences remained with an average length of 450 bp (29,852 ± 22,428 sequences/library) (Fig. S2). At both depths (mixed layer and upper-mesopelagic), there was a higher proportion of *Metazoa* affiliated sequences in SK10 and SS100, except at ICE, while a higher proportion of eukaryotic phytoplankton sequences was observed in SS0.22 and SS10 in the mixed layer (Table S1).

### *Hydrographic settings and community structure overview*

The two less productive stations were located on the Antarctic continental ice-edge (ICE) and in a high-nutrients-low-chlorophyll (HNLC) zone (P2), whereas the two more productive stations were located in a naturally iron-fertilised zone along South Georgia continental margin (P3) and in an upwelling zone at the frontal system of polar front zone and the Antarctic zone (UP) (Fig. 1). P3 and UP were in close proximity with each other and showed higher chlorophyll *a* concentrations (mean 1.90 and 1.23 µg $L^{-1}$ in the mixed layer, respectively), while ICE and P2 were further apart and had lower surface chlorophyll *a* concentrations (0.37 and 0.40 μg $L^{-1}$ respectively). There was a sharp temperature decrease between the mixed layer depth and the upper-mesopelagic at all stations except ICE, at which the surface temperature was low (< -1˚C) due to freshly melted ice (Fig. S1). At all stations, particulate organic carbon (POC) concentrations were higher in suspended particles (Table S2), and within the mixed layer depth compared to the upper-mesopelagic (Belcher et al. 2016b).

The CCA analysis based on protist OTU composition (Fig. 2) revealed a clear separation between stations, as well as between mixed layer and upper-mesopelagic samples when considering each station individually. A PERMANOVA analysis calculated for phototrophic and heterotrophic protist communities (Table S3) revealed that every environmental parameter tested (i.e., oxygen, fluorescence and POC concentrations, and temperature) as well as the particle-fraction (SK10, SS100, SS10 and SS0.22) were significant predictors of OTU composition ($p < 0.05$), the latter explaining ~ 18 % of observed variability. Similar to prokaryotic communities collected in identical particle-fractions (Duret et al. 2018), protist communities collected at ICE were the most dissimilar compared to those collected at other stations (P2, P3 and UP) (average Bray Curtis distance of 70.3 versus 56.3 % respectively) (Fig. 3). This is likely due to unique conditions present at ICE, located on the Antarctic continental ice edge (Fig. 1 and S1), compared to the other stations that were not influenced by melting-ice runoff (Atkinson et al. 2001). These conditions include negative temperatures (Chen and Laws 2017) and high concentrations of macro- (Garrison et al. 2005) and micronutrients release, such as iron and vitamin $B_{12}$ (Sedwick and Ditullio 1997; Taylor and Sullivan 2008). Such different conditions would have influenced eukaryotic phytoplankton and subsequently eukaryotic heterotrophic communities.

### ***Eukaryotic phytoplankton components of the particle flux***

*Surface eukaryotic phytoplankton communities*

Overall, diatoms (31.9 ± 25.1 %) and prymnesiophytes (28.0 ± 21.1 %), and chlorophytes at ICE (19.3 ± 13.2 %), dominated the phytoplankton communities in all particle-fractions (i.e., SK10, SS100, SS10 and SS0.22) in the mixed layer at every station (Fig. 4-A). Assuming that phytoplankton sequences detected in the mesopelagic primarily originated from sinking particles in the mixed layer, the focus for eukaryotic phytoplankton communities was placed on sinking particles (SK10) in the mixed layer for subsequent comparison with sinking and suspended particles in the upper-mesopelagic – in order to explore how phytoplankton components evolve with particle dynamics upon sinking. Expectedly, eukaryotic phytoplankton communities (≥ 10 µm) collected in the mixed layer differed largely between stations (Fig 4 A and Fig. S3), likely reflecting the different productivity regimes (Fig. 1). The less productive, iron-depleted HNLC station P2 was largely dominated by the prymnesiophyte *Phaeocystis*, representing 83.3 % of eukaryotic phytoplankton sequences of SK10 in the mixed layer, which is consistent with literature. *Phaeocystis antarctica* is one of the most prevalent phytoplankton genera in the Southern Ocean, which has been reported within sea-ice (Brown and Bowman 2001) and to form large blooms in deeply mixed waters of the Ross Sea during the Austral summer (Arrigo 1999; Zoccarato et al. 2016).

Diatom sequences represented only 15.6 % of SK10 eukaryotic phytoplankton sequences in the mixed layer at P2, but they averaged at 69.6 ± 9.7 % in ICE, and the more productive stations P3 and UP. The polar centric diatom families *Coscinodiscophyceae* and *Mediophyceae* represented most of these sequences, the former being more abundant at ICE (34.0 versus 12.0 % at the other stations) and the latter at P2, P3 and UP (11.9 versus 42.5 % respectively). *Actinocyclus* and *Corethron* were the dominant sinking diatoms at ICE (34.0

%). Conversely, *Chaeotoceros* (13.8 %) along with unidentified members of the *Mediophyceae* family (27.5 %) were the dominant sinking species at P3 and UP. *Coscinodiscophyceae* and *Mediophyceae* diatoms have consistently been reported in polar waters (Poulton et al. 2010; Rodríguez-Marconi et al. 2015; Zoccarato et al. 2016). In particular, *Actinocyclus* (*Coscinodiscophyceae*) and *Chaetoceros* (*Mediophyceae*) have frequently been detected in polar waters naturally enriched in iron (Georges et al. 2014; Rembauville et al. 2016). This agrees with the environmental conditions present at each respective station. ICE, P3 and UP benefit from various iron inputs, unlike P2 that is located in a HNLC region (Fig. 1). While eukaryotic phytoplankton communities at ICE can use high concentrations of iron originating from melted sea-ice (Sedwick and Ditullio 1997; Taylor and Sullivan 2008), P3 and UP additionally benefit from nutrient-rich upwelled waters at the South Georgia continental margin (Atkinson et al. 2001).

*Comparison with sinking eukaryotic phytoplankton in the mesopelagic*

Eukaryotic phytoplankton sequences in SK10 communities at the two depths exhibited differences in terms of their structure and diversity (Fig 4-A, 5 and Fig. S3). *Mediophyceae* diatoms, mostly represented by *Chaetoceros*, accounted for 41.5 ± 13.0 % of eukaryotic phytoplankton sequences collected in the SK10 fraction in the upper-mesopelagic at every station, while *Coscinodiscophyceae* were mostly absent, except at P2 where they represented 13.0 % of eukaryotic phytoplankton sequences. As *Actinocyclus* (*Coscinodiscophyceae*) was present in higher relative abundance in SK10 samples in the mixed layer than in the upper-mesopelagic at ICE, P3 and UP, and similar relative abundance at P2, our data implies that few *Actinocyclus* sank out from the mixed layer. Using a similar logic, our data implies that it was mostly *Chaetoceros* that were exported to the upper-mesopelagic. This apparent differential export is in agreement with literature on carbon export owing to different diatom groups (Leblanc et al. 2018): The fast-growing *Chaetoceros* has been correlated with high carbon export to depth, while the opposite is true for *Actinocyclus* that has been reported to be negatively correlated with POC export (Tréguer et al. 2018). Although *Actinocyclus* has a large biovolume, unlike *Chaetoceros*, it does not form chains (e.g., Poulton *et al.*, 2010), which thereby leads to a reduction of its sinking velocity (Bannon and Campbell 2017). Additionally, higher grazing pressures on single *Actinocyclus* cells compared to chains of *Chaetoceros* (Hoffmann et al. 2008) could also lead to the difference observed in their carbon export potential. Larger cells are indeed more easily grazed (Smetacek et al. 2002) and chain-forming represents an effective way of protection against grazers (Pahlow et al. 1997). By increasing death rates of *Actinocyclus*, micrograzers and copepods would increase their retention and remineralisation in the mixed layer and thus limit their export to the upper-mesopelagic. This potentially explains why *Actinocyclus* did not contribute as much as *Chaetoceros* to carbon export to the upper-mesopelagic. Furthermore, the presence of *Chaetoceros* sequences in SK10 fractions agrees well with the observations of chain-forming centric diatoms via light microscopy in sinking particles collected in the upper-mesopelagic during the same cruise (Belcher *et al.* 2016).

Aggregates and faecal pellets that are ballasted by biogenic minerals, such as opals produced by diatoms, sink significantly faster than those that are not (Klaas and Archer 2002; Ploug et al. 2008). As they sink faster, particles are less susceptible to the increased remineralisation processes in the upper-mesopelagic (Martin et al. 1987) and can therefore sink deeper, leading to more efficient long-term carbon sequestration (Kwon et al. 2009). This is one of the reasons why diatoms are assumed to be more efficient carbon transporter to the deep ocean (Armstrong et al. 2002; Jin. et al. 2006) as opposed to non-ballasted phytoplankton taxa such as *Phaeocystis*.

At P2, where prymnesiophytes were most dominant in the mixed layer, fewer sequences belonging to *Phaeocystis* were retrieved in SK10 in the upper-mesopelagic compared to the mixed layer (45.5 %). This implies that despite its abundance in the mixed layer, this taxon was not as efficient as diatoms for carbon export to the deep ocean. Instead, *Phaeocystis* was observed primarily in the upper-mesopelagic small-suspended fraction (SS0.22), suggesting that although they contributed to the POM flux out of the euphotic zone to some extent, *Phaeocystis*-enriched particles were subject to higher remineralisation and thus unlikely to sink to depths below the upper-mesopelagic. *Phaeocystis* has previously been reported as a key component of POC export in polar waters (DiTullio et al. 2000), as they have the ability to form aggregates that sink rapidly out of the mixed layer (Arrigo 1999). However, during our study this eukaryotic phytoplankton appeared to contribute little to carbon transfer efficiency, especially compared to its diatom counterparts, as observed elsewhere in Antarctic waters (Lin et al. 2017). The rapid export of *Phaeocystis* out of the euphotic zone is generally related to their enhanced production of transparent exopolymer polysaccharides (TEP) (Passow et al. 2001). TEP production in *Phaeocystis* tends to increase when colonies start to die (Hong et al. 1997). However, TEP-enriched particles have a reduced density that, if they are not ballasted enough (Mari et al. 2017), they show a reduced sinking velocity or can even be buoyant (Eberlein et al. 1985).

Although some cyanobacteria sequences were also present in the same samples according to parallel 16S rRNA gene amplicon sequencing dataset, we surmise that their contribution to the phytoplankton component of the BCP would be relatively small. Cyanobacteria were only detected in low numbers in 19 out of 32 samples (Table S4 and Fig. S4-A), and appeared more enriched in mesopelagic particle-fractions (Table S4-B). Their apparent low abundance is consistent with previous report of their scarcity in the Scotia Sea (Jacques and Panouse 1991) and generally in polar waters in favour to diatoms and prymnesiophytes (Ishikawa et al. 2002; Doolittle et al. 2008; Yang et al. 2012). Therefore, eukaryotic phytoplankton appeared to be the dominant phytoplankton driver of the BCP in the Scotia Sea.

At stations P2, P3 and UP, 87.1 ± 3.4 % of eukaryotic phytoplankton sequences collected in SK10 in the upper-mesopelagic were affiliated with OTUs shared with SK10 in the mixed layer (representing 23.1 % ± 2.0 % of OTUs in the upper-mesopelagic), while at ICE only 32.0 % of sequences belonged to OTUs common between SK10 at both depths (12.8 % of OTUs) (Table 1). This suggests that, at least in P2, P3 and UP, phytoplankton diversity observed in sinking particles in the upper-mesopelagic likely originated from the mixed layer. Furthermore, in the upper-mesopelagic of every station, a similar proportion of SK10 sequences were shared with all suspended particle size-fractions (91.9 ± 5.2 % representing 11.8 ± 0.8 % of OTUs). This suggests strong interchanges between sinking and suspended particles in the upper-mesopelagic, which likely originated from particles sinking in the mixed layer. Contributors to the remaining unique OTUs may come from: *(i)* the export of small sinking particles from the surface (< 10 µm) (Dall'Olmo and Mork 2014) that would have not been sampled here, *(ii)* the presence of low-light adapted phytoplankton in the upper-mesopelagic (Jacques 1983) and/or *(iii)* the lateral export of sinking particles from adjacent mesopelagic water masses.

*Influences on suspended particles in the upper-mesopelagic*

In the upper-mesopelagic, suspended particles 10–100 µm (SS10) and > 100 µm (SS100) were largely dominated by prymnesiophytes (32.4 ± 18.9 %), mostly represented by *Phaeocystis*, and by diatoms (55.6 ± 24.7 %) mainly belonging to *Proboscia* (*Coscinodiscophyceae*) at P3, *Thalassionema* (*Fragilariophyceae*) at UP, and unidentified members of *Mediophyceae* at ICE and P2 (Fig 4-A and S3). Regardless of the station, *Phaeocystis* dominated suspended particles 0.22–10 µm (SS0.22) (44.5 ± 15.4 %).

Furthermore, every suspended particle size-fraction in the upper-mesopelagic at ICE contained high proportions of chlorophyte sequences (36.8 ± 14.0 %). Prymnesiophytes and unidentified chlorophytes were particularly enriched in each suspended particle size-fractions in the upper-mesopelagic compared to SK10 in the mixed layer (Fig. 5 and Fig. S3). Notably, the chlorophyte *Prasinophyceae* clade VIII (Viprey et al. 2008) was only present in SS0.22 samples at ICE.

Most sequences retrieved from all suspended particles in the upper-mesopelagic were common with those in sinking particles SK10 in the mixed layer at all stations (81.1 ± 8.6 %, representing 22.0 ± 6.9 % of OTUs), thus again reaffirming the fact that particles sinking from mixed layer are more likely the source for suspended particles in the upper-mesopelagic. Suspended particles in the mesopelagic can originate from *(i)* the disaggregation of sinking particles, through the action of biotic and abiotic processes (Lam and Marchal 2015), *(ii)* from in situ chemolithoautotrophic primary production in the mesopelagic (Arístegui et al. 2009), and also *(iii)* from vertical mixing or lateral transport, which lead to the introduction of suspended material from adjacent water masses (Baltar et al. 2009). As only photosynthetic primary producers are considered in this section and owing to the high proportion of shared sequences between suspended particles in the upper-mesopelagic and sinking particles at both depths, the diversity observed in suspended particles in the upper-mesopelagic would therefore originate from the surface mixed layer, i.e., likely from sinking particles disaggregation and/or vertical and lateral mixing.

Furthermore, the enrichment of prymnesiophytes, and particularly of *Phaeocystis*, in every suspended particle size-fractions, coupled with the enrichment of diatoms in sinking particles in the upper-mesopelagic, supports the differential particle dynamics observed existing between prymnesiophyte-enriched and diatom-enriched particles (Figures 4-A and 5). On the one hand, prymnesiophyte-enriched particles sinking from the mixed layer were more likely to break down into suspended particles in the upper-mesopelagic. On the other hand, diatom-enriched particles were more likely to sink faster and deeper into the ocean, owing to their larger cell-sizes and mineral ballasting. This is in agreement with the observed influence of phytoplankton community structure on carbon export (Giering et al. 2017). At ICE, the higher proportion of OTUs shared between suspended particles in the mixed layer and those in the upper-mesopelagic compared to other stations suggests a bigger influence of vertical mixing that led to the intrusion of surface suspended particles deeper in the water column. This is consistent with the chlorophyll *a* profile observed at the ICE station (Fig. S1). However, this is not in agreement with the water column stabilisation effect (Petrou et al. 2016) generally expected from Antarctic continental ice edge melted runoffs (Atkinson et al. 2001) and the mixing observed at ICE was possibly caused by regional hydrographic effects that remained to be determined.

### *Metazoan components of the particle flux*

For metazoans, our focus was placed on SK10 and SS100 where most of the larger fragments of organisms and whole organisms (> 100 μm) would have been recovered, and thus be most informative regarding their influences on sinking versus suspended particles. Metazoan sequences were most abundant in these fractions compared to SS10 (except at ICE) and SS0.22 (Table S1). Metazoan sequences recovered in SS10 and SS0.22 likely corresponded to small fragments of organisms and/or faecal pellets.

The diversity of sequences collected in SK10 in the mixed layer was similar to that of the upper-mesopelagic, as 87.5 ± 9.6 % of metazoan sequences and 19.6 ± 9.6 % of OTUs were shared between the two particle pools (Table 1). Nonetheless, the compositions of metazoan sequences in SK10 at the two depths were different (Fig. 4-B and S5). Except in the mixed layer at ICE, SK10 samples were dominated by copepod sequences (90.4 ± 5.1 %), which were mostly affiliated with *Calanoida* (67.6 ± 6.7 %) and *Cyclopoida* (20.9 ± 6.0 %). This agrees with results from Belcher et al. (2016) that attributed more than half of sinking POC flux at this station to calanoid faecal pellets. Due to their relatively fast sinking, POC export dominated by mesozooplankton faecal pellets generally leads to limited connectivity between sinking and suspended particle pools in the mesopelagic. Faecal pellets are indeed more resistant to remineralisation compared to phytoplankton-dominated particles and conferred low microbial respiration rates (Belcher et al., 2016), as they have higher densities and are surrounded by a protective membrane (Abramson et al. 2010). Beside their role in repackaging surface primary production into faecal pellets (Turner 2015), mesozooplankton are also responsible for the breakage of sinking particles (e.g., sloppy feeding [Steinberg and Landry, 2017], microbial gardening [Mayor et al. 2014]) and contribute to the creation of smaller suspended particles, thereby connecting the two particle-pools together (Lam and Marchal 2015).

In the upper-mesopelagic, sequences retrieved from SS100 and SK10 at ICE and P3 showed slightly enhanced differences compared to those from P2 and UP (Table 1). While SK10 at ICE and P3 were dominated by copepod sequences (> 80.0 %), SS100 was dominated by sequences that belonged to the more soft-bodied organisms, including the tunicate family *Oikopleuridae* at ICE, while at P3 *Oikopleuridae,* the ctenophore class *Typhlocoela* and cnidarian class *Trachylinae*. Such distinction suggests different roles played by mesozooplankton taxa in sinking and suspended particle-pools within the upper-mesopelagic ocean.

The main limitations of these results are that *(i)* living copepods could have swum towards the bottom of the MSC to feed on sinking particles within the time frame of particle settling

(2 hours), which would subsequently have reduced their detection in suspended particles (i.e., in the upper part of the MSC); and that *(ii)* the exact source of detected DNA is difficult to determine. That is, the DNA collected could indicate the presence of the organisms (e.g., copepods) themselves while alive, or merely fragments of shredded or dead body parts (e.g., antennas, broken shells), residual genetic materials present in faecal pellets, or allochthonous materials advected into the sampled site and depth. Nonetheless, these results indicated that while copepods were more influential on sinking particles, either with their faecal pellets or by their feeding behaviours, the soft-bodied *Oikopleuridae*, *Typhlocoela* and *Trachylinae* were more important for suspended particles, especially in the more productive stations. Suspended particles could represent an organic substrate for these animals, as it was suggested in the central North Pacific (Gloeckler et al. 2017). Alternatively, their soft-tissue structures and/or secretions could actually be a major component of suspended particles themselves acting as a binder for smaller particles and dissolved organic matter, similar to empty larvacean houses, without ever reaching densities high enough to sink as is sometimes observed (Alldredge 1976; Simon et al. 2002; Wilson et al. 2008).

The use of 18S rRNA gene amplicon sequencing to investigate the contribution of metazoans to suspended and sinking particles represents a useful complement to classic microscopic analyses, which usually focuses only on large, sinking particles, and is limited by recognisable morphologies of body parts, often missing the smaller and amorphous fragments. Our amplicon sequencing approach shares the same metabarcoding principle as the increasingly applied environment DNA (eDNA) approach (Thomsen et al. 2012; Andruszkiewicz et al. 2017; Flaviani et al. 2017; Djurhuus et al. 2018). They also share the same limitations by the degree of quantitative information the data could convey, due PCR biases and different amounts of DNA or gene copies present in the organisms (part or whole) concerned.

### ***Heterotrophic protists and fungi associated with particles***

#### *Community connectivity with depth and method limitations*

Given their high numerical abundances and various trophic modes (Sherr and Sherr 2002; Worden et al. 2015; Stoecker et al. 2017), such as in polar environments (Korb et al. 2012; Caron et al. 2016), heterotrophic protists are key players in the remineralisation and cycling of organic matter. The abundances of specific groups of heterotrophic protists varied among sampled stations and depths, which were likely influenced by the inherent environmental conditions (Fig. 2) and reflected a geographic niche specialisation amongst heterotrophic protists as has been observed in various oceanic environments (Williams et al. 2018). Nonetheless, OTU composition was mainly driven by the particle-fraction which explained 18.4 % of OTU variability ($p < 0.05$) (Table S3). Heterotrophic protist communities in the mixed layer were on average 43.2 ± 15.1 % dissimilar compared to 58.5 ± 14.9 % in the upper-mesopelagic (Table S5). Every particle-fraction in the upper-mesopelagic was on average 66.6 ± 13.6 % dissimilar compared to SK10 in the mixed layer. This agrees with the literature showing that heterotrophic protist assemblages from the surface differ from those from the mesopelagic and deeper (López-García et al. 2001; Edgcomb et al. 2011; Orsi et al. 2012; Pernice et al. 2014, 2015; Duret et al. 2015; Zoccarato et al. 2016). However, heterotrophic protist communities in the mesopelagic ocean and below remain largely unknown (Edgcomb 2016; Caron 2017), especially in the Southern Ocean, despite the fact that most POC flux attenuation and so remineralisation typically occurs within the mesopelagic (Martin et al. 1987). In order to get an insight into the roles of heterotrophic protists in remineralisation processes and particle dynamics processes where they are most active, the following section focuses on differences between particle-fractions collected in the upper-mesopelagic.

In the meso- and bathypelagic, ciliates are scarce (Arístegui et al. 2009; Morgan-Smith et al. 2013; Bochdansky et al. 2017) compared to heterotrophic nanoflagellates (e.g., Tanaka and Rassoulzadegan 2002; Gowing et al. 2003; Pernice et al. 2014; Dolan et al. 2017). Despite nanoflagellates biomass sometimes exceeding that of ciliates (Safi et al. 2012), the latter usually dominate the relative abundance of 18S rRNA gene amplicon sequencing datasets (e.g., Countway et al. 2005; Duret et al. 2015; Pernice et al. 2015) owing to high numbers of SSU rRNA gene copies and DNA content (Zhu et al. 2005; Gong et al. 2013). The accurate quantitative detection of other alveolates, such as dinoflagellates (Godhe et al. 2008), and rhizarians, i.e., radiolarians (Suzuki and Aita 2011) and collodarians (Biard et al. 2017); present similar limitations owing to high numbers of gene copies.

*Alveolata* were the most abundant taxa among all samples in our dataset (Fig. 3), representing 84.7 ± 13.0 % of heterotrophic sequences. While *Dinoflagellata* sequences were relatively abundant in all particle-fractions (37.5 ± 18.3 %), the parasitic *Protalveolata* sequences were most abundant in SS0.22 (34.0 ± 9.9 % versus 5.7 ± 2.6 % in other particle-fractions) and *Ciliophora* sequences were most abundant in SS100, SS10 and SK10 (21.5 ± 8.7 % versus 5.0 ± 1.5 % in SS0.22) (Fig. S6-A and S6-B, Table S1). Although ciliates (Caron et al. 1982; Silver et al. 1998; Gowing et al. 2001) and radiolarians (Lampitt et al. 2009; Biard et al. 2016) have been reported associated with particles in the mesopelagic, our dataset does not accurately inform on their true abundance compared to smaller heterotrophs that are equally important in top-down control of phytoplankton and bacterial communities in cold waters (Garzio et al. 2013). Relative abundances presented below were normalised within each category (i.e., dinoflagellates, choanoflagellates, *Syndiniales*, ciliates, rhizarians and fungi) (Fig. 6) in order to better visualised differences between less represented taxa.

*Flagellates*

While certain dinoflagellates taxonomic groups were enriched in specific particle-fractions, differences between stations were important. *Gymnodiniales* sequences were overall least abundant at ICE (2.19 ± 1.58 %) than at P2 (9.98 ± 3.14 %), and were less represented in SS100 than other particle-fractions. Different *Gyrodinium* species (*Gymnodiniaceae*) were enriched in specific particle-fractions, with *Gyrodinium fusiforme* most abundant in SS10 and SK10 at P2, *Gyrodinium rubrum* in SK10, and unidentified *Gyrodinium* spp. in SS0.22. *Gyrodinium* cells (10 to 100 µm) are able to feed on phytoplankton cells much bigger than themselves, such as diatoms (Sherr and Sherr 2007). They have thus been negatively correlated with POC export in the Southern Ocean owing to their grazing activities (Cassar et al. 2015; Lin et al. 2017). *Gymnodinium* spp. was most enriched in SS10, and *Gymnodinium aureolum* was most enriched in SS0.22. These unarmoured dinoflagellates can either be autotrophic, such as *Gymnodinium aureolum*, forming blooms (Garrison et al. 2005; Jeong et al. 2010), or ectoparasites (Gómez et al. 2009). The recovery of *Gymnodinium aureolum* in SS0.22 could correspond to cells living freely in the water column, while those recovered in SS10 could correspond to parasitic species. A crustacean eggs ectoparasite *Chytriodinium roseum* (Gómez et al. 2009) was however most abundant in SS0.22. The copepod parasite genera *Blastodinium* spp. (Skovgaard et al. 2012) was well represented in SK10 and SS100, and likely correspond to dinoflagellates hosted by copepods recovered in these larger size-fractions (≥ 100 µm).

*Peridiniales* sequences were most abundant in SK10 and SS100. Two cold water ubiquitous predatory motile flagellates *Islandinium tricingulatum* and *Protoperidinium pellucidum* (Okolodkov 1999; Head et al. 2001) were most abundant in SK10. Furthermore, the ubiquitous predatory *Phalachroma* spp. (*Dinophysiales* - *Oxyphysiaceae*) (Jensen and Daugbjerg 2009) was most abundant in SK10 at all stations.

Choanoflagellates (*Holozoa*) sequences were mostly represented by the taxonomic family *Stephanoecidae* (*Acanthoecida*), belonging mostly to *Diaphanoeca grandis* in SS100 and by group H in SK10 and SS10. *Stephanoecidae* choanoflagellates are ubiquitous bacterivorous predators (Marchant 1985) measuring between 3 and 10 µm (Kirchman 2008) that are regularly detected in polar waters (Smith et al. 2011; Georges et al. 2014). Their detection in larger particle size-fractions suggests an active colonisation by these nanoflagellates of sinking and suspended particles ≥ 100 µm. Alternatively, their detection could be indicative of colony formation (Thomsen et al. 1991). Sequences from the choanoflagellates family *Monosigidae* group B (*Craspedida*) sequences from were only detected at ICE, mostly in SK10.

Parasitic *Syndiniales* sequences are commonly detected in 18S rRNA gene sequencing in high abundances (e.g., Sauvadet et al. 2010; de Vargas et al. 2015; Cleary and Durbin 2016; Gutierrez-Rodriguez et al. 2019a). They affect a wide variety of hosts, ranging from diatoms (Berdjeb *et al.*, 2018), tintinnides (Harada et al. 2007), radiolarians (Dolven et al. 2007) to copepods (Skovgaard *et al.*, 2005). Sequences belonging to the parasitic *Syndiniales* showed strong enrichment patterns. SS10 was most enriched in group I clade 8, SS100 in group II clade 10 + 11 as well as group I clade 8. SS0.22 was most enriched in group II clade 10 + 11 and clade 7. The latter clade has been mostly recovered in aphotic layers and is hypothesised to be affecting radiolarians in the mesopelagic (Guillou et al. 2008). The detection of *Syndiniales* group II has been reported in the small fraction of Antarctic waters previously (López-García et al. 2001), and could correspond to the detection of dinospores (1-12 µm) dispersed in the water column (Guillou et al. 2008). Group I has been recovered from anoxic and suboxic samples more systematically than group II (Guillou et al. 2008), and their detection mostly in suspended particles ≥ 10 µm could indicate the presence reduced conditions in this particle-pool. SK10 had a more diverse composition, that could indicate more transient conditions and/or the presence of a variety of hosts associated with sinking particles.

Although represented within each particle-fractions, most predatory flagellate sequences were recovered in sinking particles. These predators likely feed on sinking particle-associated bacterial populations (Fenchel 1982a; b; c; Sherr and Sherr 2002) and phytoplanktonic cells within particles (Sherr and Sherr 2007). Their more important detection on sinking particles could reflect the presence of their preferred bacterial prey (e.g., Anderson et al. 2013) which would be in agreement with the differential bacterial communities associated with sinking and suspended particles collected during the same cruise (Duret et al. 2018). Additionally, their detection in sinking particles rather than in other large suspended particles might have been artificially created in the marine snow catcher by the creation of a chemical gradient as particle sank to the bottom of the sampler, which would have cause them to preferentially colonise these particles by chemotaxis (Fenchel 2001). It is nonetheless important to keep in mind that most dinoflagellates sequences could not be annotated at a high taxonomic resolution under PR$^2$ or Silva (representing 91.8 ± 5.1 % of dinoflagellates sequences) and could correspond to predatory species.

*Ciliates*

Ciliate sequences did not present evident enrichment patterns in sinking or suspended particles ≥ 10 µm, suggesting that their detection reflected their cell sizes (generally > 40 µm) and/or their attachment to both particle-fractions > 100 µm. These predators likely act in the top-down controls of bacterial prey populations associated with suspended and sinking particles (Caron et al. 2012). Nonetheless, sequences affiliated with *Tintinnida* and *Litostomatea* at P2 were slightly more abundant in SK10 than other particle-fractions, both of which have previously been detected in various mesopelagic sites (e.g., Grattepanche et al. 2016; Zoccarato et al. 2016; Dolan et al. 2017). Furthermore, sequences belonging to OLIGO5 (*Oligohymenophorea*) and *Discotrichidae* (*Nassophorea*) were slightly more abundant in SS0.22 at most stations.

Most ciliate sequences were affiliated with *Choreotrichida* and *Strombidiida* (*Spirotrichea*) in every samples. These sequences were mainly represented by *Leegaardiella* sp. and *Strombidium* sp. respectively, the latter being mainly present at P2. Both genus include heterotrophic and mixotrophic species that have been reported to be important components of the ciliate communities in Arctic waters (Jiang et al. 2015). While *Leegaardiella* sp. are mainly reported to be heterotrophic, *Strombidium* sp. are mostly mixotrophs (Dziallas et al. 2012) that have the ability to sequester chloroplasts from their phytoplankton prey (i.e., kleptoplastidy) and can therefore participate in primary production when light conditions allow (Stoecker et al. 2017).

*Rhizarian*

Unsurprisingly, most *Rhizaria* sequences belonged to radiolarians. Radiolarians are globally abundant in the mesopelagic ocean, where they represent a large proportion of the planktonic biomass (Biard et al. 2016; Boltovskoy and Correa 2016). These mostly mixotrophic organisms (Caron et al. 2012; Decelle et al. 2012; Flynn et al. 2013; Stoecker et al. 2017) are key components to the transfer of organic matter to the deep-ocean, owing to their large cell sizes (40 to 400 µm) (Suzuki and Aita 2011) and their mineral exoskeleton acting as ballast, and are regularly detected in sediment traps (e.g., Boyd and Trull 2007; Lampitt et al. 2009; Biard et al. 2018; Gutierrez-Rodriguez et al. 2019). Radiolarian sequences exhibited strong enrichment patterns in specific particle-fractions. On the one hand, silica bearing radiolarians sequences (Suzuki and Not 2015) were most enriched in suspended particles, with RAD C most enriched in suspended particles ≥ 10 µm and RAD B in SS0.22. On the other hand, strontium sulphate bearing acantharians (Decelle et al. 2013) were most abundant in SK10, represented by *Symphyacanthida* at P3 and ICE, *Chaunacanthida* at P2, P3, and group VI at P2. These sequences could correspond to acantharian cysts, generally measuring up to 1 mm, which have been reported to participate to organic carbon export to depth (Decelle et al. 2013). Furthermore, sequences belonging to the heterotrophic *Phaeodaria* group were mostly enriched in SK10 and represented by *Protocystis* sp. This which is also consistent with studies conducted in other oceanic regions, where they play an important role in organic carbon export (Biard et al. 2018; Stukel et al. 2018).

The differential enrichment of radiolarians in suspended and sinking particles could reflect various efficiencies in carbon export from the mixed-layer to the upper mesopelagic between groups, with acantharians being more efficient than RAD B and C. Additionally, these differences could correspond to differential life-stages (e.g., cyst, vegetative cell, free-living cell) or physiological state (heterotrophy or autotrophy).

### *Fungi*

Rather than presenting enrichment patterns among particle-fractions, fungi sequences presented most differences between stations. The sporous *Microbotryomycetes* (*Basidiomycota* - *Pucciniomycotina*) and filamentous *Dothideomycetes* (*Ascomycota* - *Pezizomycotina*) were most enriched at ICE, while the sporous *Chytridiomycetes* (*Chytridiomycota* - *Chytridiomycotina*) and *Exobasidiomycetes* (*Basidiomycota* - *Ustilaginomycotina*) were most enriched at P3 and UP. *Basidiomycota*, *Ascomycota* and *Chytridiomycota* have been reported previously in frozen Antarctic lakes (Gonçalves et al.

2012; Rojas-Jimenez et al. 2017). Marine fungi have been reported to play important roles in organic matter degradation in upwellings (off the coast of Chile; Gutiérrez et al. 2010, 2011) and in particles in coastal regions (Taylor and Cunliffe 2016) and in the bathypelagic (Bochdansky et al. 2017). It is however difficult to conclude regarding their role within particles collected at the different stations, as they could either be heterotrophic or parasitic (Grossart et al. 2019).

## Conclusion

This study provides the first insights into eukaryotic contribution to suspended and sinking particle-pools in the mixed layer and the upper-mesopelagic of the Scotia Sea. Amplicon sequencing of the 18S rRNA gene served as a powerful diagnostic tool to identify the major eukaryotic phytoplankton present in sinking particles that most likely drives the biological carbon pump strength, and gave insights into the influence of metazoans, heterotrophic protists and fungi on sinking and suspended particles in the upper-mesopelagic. Notably, the chain-forming genus *Chaetoceros* dominated the eukaryotic phytoplankton component of sinking particles thereby suggesting that they facilitated carbon flux out of the mixed layer to the upper-mesopelagic. Prymnesiophyte-enriched particles appeared to be more easily broken down into suspended particles in the upper-mesopelagic, conferring lower transfer efficiency to the biological carbon pump. Copepods, either by their feeding behaviour and/or the production of dense faecal pellets, were more influential on sinking particles than on suspended particles; while at some stations soft-tissue organisms were found to primarily affect suspended particles. Heterotrophic protists and fungi communities in the upper-mesopelagic resembled little to their mixed-layer counterparts. The distinct community structures observed in various particle-fractions suggests different ecological conditions existing within suspended and sinking particles, such as chemical composition of organic matter and prey population availability. Nonetheless, investigations into predator-prey specificities, organic matter requirements, as well as quantification of these heterotrophic groups are required to further understand their effects on suspended and sinking particles, as well as to decipher their respective roles in the biological carbon pump. Results from this study further highlight the need to consider, the interactions of eukaryotic communities with both sinking and suspended particles, along with the respective prokaryotic communities, when evaluating the strengths and controls of the biological carbon pump.

## References


Abramson, L., C. Lee, Z. Liu, S. G. Wakeham, and J. Szlosek. 2010. Exchange between suspended and sinking particles in the northwest Mediterranean as inferred from the organic composition of in situ pump and sediment trap samples. Limnol. Oceanogr. **55**: 725–739. doi:10.4319/lo.2009.55.2.0725

Alldredge, A. L. 1976. Discarded appendicularian houses as sources of food, surface habitats, and particulate organic matter in planktonic environments. Limnol. Oceanogr. **21**: 14–24. doi:10.4319/lo.1976.21.1.0014

Anderson, R., C. Wylezich, S. Glaubitz, M. Labrenz, and K. Jürgens. 2013. Impact of protist grazing on a key bacterial group for biogeochemical cycling in Baltic Sea pelagic oxic/anoxic interfaces. Environ. Microbiol. **15**: 1580–1594. doi:10.1111/1462-2920.12078

Andruszkiewicz, E. A., H. A. Starks, F. P. Chavez, L. M. Sassoubre, B. A. Block, and A. B. Boehm. 2017. Biomonitoring of marine vertebrates in Monterey Bay using eDNA metabarcoding. PLoS One **12**: 1–20. doi:10.1371/journal.pone.0176343

Arístegui, J., J. M. Gasol, C. M. Duarte, and G. J. Herndld. 2009. Microbial oceanography of the dark ocean’s pelagic realm. Limnol. Oceanogr. **54**: 1501–1529. doi:10.4319/lo.2009.54.5.1501

Armstrong, R. a., C. Lee, J. I. Hedges, S. Honjo, and S. G. Wakeham. 2002. A new, mechanistic model for organic carbon fluxes in the ocean based on the quantitative association of POC with ballast minerals. Deep. Res. Part II Top. Stud. Oceanogr. **49**: 219–236. doi:10.1016/S0967-0645(01)00101-1

Arrigo, K. R. 1999. Phytoplankton Community Structure and the Drawdown of Nutrients and

$CO_2$ in the Southern Ocean. Science (80-. ). **283**: 365–367. doi:10.1126/science.283.5400.365

Atkinson, A., M. J. Whitehouse, J. Priddle, G. C. Cripps, P. Ward, and M. A. Brandon. 2001. South Georgia, Antarctica: A productive, cold water, pelagic ecosystem. Mar. Ecol. Prog. Ser. **216**: 279–308. doi:10.3354/meps216279

Bacon, M. P., C. A. Huh, A. P. Fleer, and W. G. Deuser. 1985. Seasonality in the flux of natural radionuclides and plutonium in the deep Sargasso Sea. Deep Sea Res. Part A, Oceanogr. Res. Pap. **32**: 273–286. doi:10.1016/0198-0149(85)90079-2

Baker, C. A., S. A. Henson, E. L. Cavan, and others. 2017. Slow-sinking particulate organic carbon in the Atlantic Ocean: magnitude, flux and potential controls. Global Biogeochem. Cycles 1–15. doi:10.1002/2017GB005638

Baltar, F., J. Arístegui, J. M. Gasol, E. Sintes, and G. J. Herndl. 2009. Evidence of prokaryotic metabolism on suspended particulate organic matter in the dark waters of the subtropical North Atlantic. Limnol. Oceanogr. **54**: 182–193. doi:10.4319/lo.2009.54.1.0182

Baltar, F., J. Arístegui, E. Sintes, J. M. Gasol, T. Reinthaler, and G. J. Herndl. 2010. Significance of non-sinking particulate organic carbon and dark $CO_2$ fixation to heterotrophic carbon demand in the mesopelagic northeast Atlantic. Geophys. Res. Lett. **37**: 1–6. doi:10.1029/2010GL043105

Bannon, C. C., and D. A. Campbell. 2017. Sinking towards destiny: High throughput measurement of phytoplankton sinking rates through time-resolved fluorescence plate spectroscopy. PLoS One **12**: 1–16. doi:10.1371/journal.pone.0185166

Belcher, A., M. Iversen, S. Giering, V. Riou, S. Henson, and R. Sanders. 2016a. Depthresolved particle associated microbial respiration in the northeast Atlantic. Biogeosciences Discuss. 1–31. doi:10.5194/bg-2016-130

Belcher, A., M. Iversen, C. Manno, S. A. Henson, G. A. Tarling, and R. Sanders. 2016b. The role of particle associated microbes in remineralization of fecal pellets in the upper mesopelagic of the Scotia Sea, Antarctica. Limnol. Oceanogr. **61**: 1049–1064. doi:10.1002/lno.10269

Berdjeb, L., A. Parada, D. M. Needham, and J. A. Fuhrman. 2018. Short-term dynamics and interactions of marine protist communities during the spring – summer transition. ISME J. doi:10.1038/s41396-018-0097-x

Biard, T., E. Bigeard, S. Audic, J. Poulain, A. Gutierrez-Rodriguez, S. Pesant, L. Stemmann, and F. Not. 2017. Biogeography and diversity of Collodaria (Radiolaria) in the global ocean. ISME J. **11**: 1331–1344. doi:10.1038/ismej.2017.12

Biard, T., J. W. Krause, M. R. Stukel, and M. D. Ohman. 2018. The Significance of Giant Phaeodarians (Rhizaria) to Biogenic Silica Export in the California Current Ecosystem. Global Biogeochem. Cycles **32**: 987–1004. doi:10.1029/2018GB005877

Biard, T., L. Stemmann, M. Picheral, and others. 2016. In situ imaging reveals the biomass of giant protists in the global ocean. Nature **532**: 504–507. doi:10.1038/nature17652

Bishop, J. K. B., J. M. Edmond, D. R. Ketten, M. P. Bacon, and W. B. Silker. 1977. The chemistry, biology, and vertical flux of particulate matter from the upper 400 m of the equatorial Atlantic Ocean. Deep Sea Res. **24**: 511–548. doi:10.1016/0146-6291(77)90526-4

Bochdansky, A. B., H. M. van Aken, and G. J. Herndl. 2010. Role of macroscopic particles in deep-sea oxygen consumption. Proc. Natl. Acad. Sci. U. S. A. **107**: 8287–8291.

doi:10.1073/pnas.0913744107

Bochdansky, A. B., M. A. Clouse, and G. J. Herndl. 2017. Eukaryotic microbes, principally fungi and labyrinthulomycetes, dominate biomass on bathypelagic marine snow. ISME J. **11**: 362–373. doi:10.1038/ismej.2016.113

Boltovskoy, D., and N. Correa. 2016. Biogeography of Radiolaria Polycystina (Protista) in the World Ocean. Prog. Oceanogr. **149**: 82–105. doi:10.1016/j.pocean.2016.09.006

Boyd, P. W., and T. W. Trull. 2007. Understanding the export of biogenic particles in oceanic waters: Is there consensus? Prog. Oceanogr. **72**: 276–312. doi:10.1016/j.pocean.2006.10.007

Brown, M. V., and J. P. Bowman. 2001. A molecular phylogenetic survey of sea-ice microbial communities (SIMCO). FEMS Microbiol. Ecol. **35**: 267–275. doi:10.1016/S0168-6496(01)00100-3

Buesseler, K. O., and P. W. Boyd. 2009. Shedding light on processes that control particle export and flux attenuation in the twilight zone of the open ocean. Limnol. Oceanogr. **54**: 1210–1232. doi:10.4319/lo.2009.54.4.1210

Calbet, A., and M. R. Landry. 2004. Phytoplankton growth, microzooplankton grazing, and carbon cycling in marine systems. Limnol. Oceanogr. **49**: 51–57. doi:10.4319/lo.2004.49.1.0051

Caporaso, J. G., C. L. Lauber, W. A. Walters, D. Berg-lyons, C. A. Lozupone, P. J. Turnbaugh, N. Fierer, and R. Knight. 2010. Global patterns of 16S rRNA diversity at a depth of millions of sequences per sample. Proc. Natl. Acad. Sci. U. S. A. **108**: 4516–4522. doi:10.1073/pnas.1000080107/-/DCSupplemental.www.pnas.org/cgi/doi/10.1073/pnas.1000080107

Caron, D. A. 2017. Acknowledging and incorporating mixed nutrition into aquatic protistan ecology, finally. Environ. Microbiol. Rep. **9**: 41–43. doi:10.1111/1758-2229.12514

Caron, D. A., P. D. Countway, A. C. Jones, D. Y. Kim, and A. Schnetzer. 2012. Marine Protistan Diversity. Ann. Rev. Mar. Sci. **4**: 467–493. doi:10.1146/annurev-marine-120709-142802

Caron, D. A., P. G. Davis, L. P. Madin, and J. M. Sieburth. 1982. Heterotrophic Bacteria and Bacterivorous Protozoa in Oceanic Macroaggregates. Science (80-. ). **218**: 795–797. doi:10.1126/science.218.4574.795

Caron, D. A., R. J. Gast, and M. È. Garneau. 2016. Sea ice as a habitat for micrograzers. Sea Ice Third Ed. 370–393. doi:10.1002/9781118778371.ch15

Cassar, N., S. W. Wright, P. G. Thomson, and others. 2015. Global Biogeochemical Cycles composition in the Southern Ocean. Global Biogeochem. Cycles 1–17. doi:10.1002/2014GB004936.Received

Cavan, E. L., F. A. C. Le Moigne,  a J. Poulton, G. a Tarling, P. Ward, C. J. Daniels, G. M. Fragoso, and R. J. Sanders. 2015. Attenuation of particulate organic carbon flux in the Scotia Sea, Southern Ocean, is controlled by zooplankton fecal pellets. Geophys. Res. Lett. **42**: 821–830. doi:10.1002/2014GL062744

Cavan, E. L., M. Trimmer, F. Shelley, and R. Sanders. 2017. Remineralization of particulate organic carbon in an ocean oxygen minimum zone. Nat. Commun. **8**: 1–9. doi:10.1038/ncomms14847

Chen, B., and E. A. Laws. 2017. Is there a difference of temperature sensitivity between marine phytoplankton and heterotrophs? Limnol. Oceanogr. **62**: 806–817. doi:10.1002/lno.10462

Cho, B. C., and F. Azam. 1988. Major role of bacteria in biogeochemical fluxes in the ocean’s interior. Nature **332**: 441–443. doi:10.1038/332441a0

Cleary, A. C., and E. G. Durbin. 2016. Unexpected prevalence of parasite 18S rDNA sequences in winter among Antarctic marine protists. J. Plankton Res. **38**: 401–417. doi:10.1093/plankt/fbw005

Collins, J. R., B. R. Edwards, K. Thamatrakoln, J. E. Ossolinski, G. R. DiTullio, K. D. Bidle, S. C. Doney, and B. A. S. Van Mooy. 2015. The multiple fates of sinking particles in the North Atlantic Ocean. Global Biogeochem. Cycles **29**: 1471–1494. doi:10.1002/2014GB005037

Countway, P. D., R. J. Gast, P. Savai, and D. A. Caron. 2005. Protistan diversity estimates based on 18S rDNA from seawater incubations in the Western North Atlantic. J. Eukaryot. Microbiol. **52**: 95–106. doi:10.1111/j.1550-7408.2005.05202006.x

Crespo, B. G., T. Pommier, B. Fernández-Gómez, and C. Pedrós-Alió. 2013. Taxonomic composition of the particle-attached and free-living bacterial assemblages in the Northwest Mediterranean Sea analyzed by pyrosequencing of the 16S rRNA. Microbiologyopen **2**: 541–552. doi:10.1002/mbo3.92

Dall’Olmo, G., and K. A. Mork. 2014. Carbon export by small particles in the Norwegian Sea. Geophys. Res. Lett. **41**: 2921–2927. doi:10.1002/2014GL059244

Decelle, J., P. Martin, K. Paborstava, and others. 2013. Diversity, Ecology and Biogeochemistry of Cyst-Forming Acantharia (Radiolaria) in the Oceans L.J. Stal [ed.]. PLoS One **8**: e53598. doi:10.1371/journal.pone.0053598

Decelle, J., I. Probert, L. Bittner, and others. 2012. An original mode of symbiosis in open ocean plankton. Proc. Natl. Acad. Sci. **109**: 18000–18005.

doi:10.1073/pnas.1212303109

Delong, E. F., D. G. Franks, and A. L. Alldredge. 1993. Phylogenetic diversity of aggregate-attached vs. free-living marine bacterial assemblages. Limnol. Oceanogr. **38**: 924–934. doi:10.4319/lo.1993.38.5.0924

DiTullio, G. R., J. M. Grebmeier, K. R. Arrigo, and others. 2000. Rapid and early export of Phaeocystis antarctica blooms in the Ross Sea, Antarctica. Nature **404**: 595–598. doi:10.1038/35007061

Djurhuus, A., K. Pitz, N. A. Sawaya, J. Rojas-Márquez, B. Michaud, E. Montes, F. Muller-Karger, and M. Breitbart. 2018. Evaluation of marine zooplankton community structure through environmental DNA metabarcoding. Limnol. Oceanogr. Methods 209–221. doi:10.1002/lom3.10237

Dolan, J. R., M. Ciobanu, S. Marro, and L. Coppola. 2017. An exploratory study of heterotrophic protists of the mesopelagic Mediterranean Sea. ICES J. Mar. Sci. doi:10.1093/icesjms/fsx218

Dolven, J. K., C. Lindqvist, V. A. Albert, K. R. Bjørklund, T. Yuasa, O. Takahashi, and S. Mayama. 2007. Molecular Diversity of Alveolates Associated with Neritic North Atlantic Radiolarians. Protist **158**: 65–76. doi:10.1016/j.protis.2006.07.004

Doolittle, D. F., W. K. W. Li, and A. M. Wood. 2008. Wintertime abundance of picoplankton in the Atlantic sector of the Southern Ocean. Nov. Hedwigia **Suppl. 133**: 147–160. doi:1438-9134/08/0133–147

Duret, M. T., R. S. Lampitt, and P. Lam. 2018. Prokaryotic niche partitioning between suspended and sinking marine particles. Environ. Microbiol. Rep. **00**: 1–15. doi:10.1111/1758-2229.12692

Duret, M. T., M. G. Pachiadaki, F. J. Stewart, N. Sarode, U. Christaki, S. Monchy, A. Srivastava, and V. P. Edgcomb. 2015. Size-fractionated diversity of eukaryotic microbial communities in the Eastern Tropical North Pacific oxygen minimum zone. FEMS Microbiol. Ecol. **91**: fiv037–fiv037. doi:10.1093/femsec/fiv037

Dziallas, C., M. Allgaier, M. T. Monaghan, and H. P. Grossart. 2012. Act together-implications of symbioses in aquatic ciliates. Front. Microbiol. **3**: 1–17. doi:10.3389/fmicb.2012.00288

Eberlein, K., M. Leal, K. Hammer, and W. Hickel. 1985. Dissolved organic substances during a Phaeocystis pouchetii bloom in the German Bight (North Sea). Mar. Biol. **316**: 311–316. doi:10.1038/470444a

Ebersbach, F., T. W. Trull, D. M. Davies, and S. G. Bray. 2011. Controls on mesopelagic particle fluxes in the Sub-Antarctic and Polar Frontal Zones in the Southern Ocean south of Australia in summer-Perspectives from free-drifting sediment traps. Deep. Res. Part II Top. Stud. Oceanogr. **58**: 2260–2276. doi:10.1016/j.dsr2.2011.05.025

Edgcomb, V., W. Orsi, J. Bunge, and others. 2011. Protistan microbial observatory in the Cariaco Basin, Caribbean. I. Pyrosequencing vs Sanger insights into species richness. ISME J. **5**: 1344–56. doi:10.1038/ismej.2011.6

Edgcomb, V. P. 2016. Marine protist associations and environmental impacts across trophic levels in the twilight zone and below. Curr. Opin. Microbiol. **31**: 169–175. doi:10.1016/j.mib.2016.04.001

Fenchel, T. 1982a. Ecology of heterotrophic microflagellates. I. Some important forms and their functional morphology. Mar. Ecol. Prog. Ser. Oldend. **8**: 211–223.

Fenchel, T. 1982b. Ecology of Heterotrophic Microflagellates. II. Bioenergetics and Growth.

Mar. Ecol. Prog. Ser. **8**: 225–231.

Fenchel, T. 1982c. Ecology of heterotrophic microflagellates. III. Adaptations to heterogeneous environments. Mar. Ecol. Prog. Ser **9**: 25–33.

Fenchel, T. 2001. How Dinoflagellates Swim. Protist **152**: 329–338. doi:10.1078/1434-4610-00071

Flaviani, F., D. C. Schroeder, C. Balestreri, J. L. Schroeder, K. Moore, K. Paszkiewicz, M. C. Pfaff, and E. P. Rybicki. 2017. A pelagic microbiome (Viruses to protists) from a small cup of seawater. Viruses **9**. doi:10.3390/v9030047

Flynn, K. J., D. K. Stoecker, A. Mitra, J. A. Raven, P. M. Glibert, P. J. Hansen, E. Granéli, and J. M. Burkholder. 2013. Misuse of the phytoplankton-zooplankton dichotomy: The need to assign organisms as mixotrophs within plankton functional types. J. Plankton Res. **35**: 3–11. doi:10.1093/plankt/fbs062

Francois, R., S. Honjo, R. Krishfield, and S. Manganini. 2002. Factors controlling the flux of organic carbon to the bathypelagic zone of the ocean. Global Biogeochem. Cycles **16**: 34-1-34–20. doi:10.1029/2001GB001722

Garrison, D. L., A. Gibson, S. L. Coale, M. M. Gowing, Y. B. Okolodkov, C. H. Fritsen, and M. O. Jeffries. 2005. Sea-ice microbial communities in the Ross Sea: Autumn and summer biota. Mar. Ecol. Prog. Ser. **300**: 39–52. doi:10.3354/meps300039

Garzio, L. M., D. K. Steinberg, M. Erickson, and H. W. Ducklow. 2013. Microzooplankton grazing along the Western Antarctic Peninsula. Aquat. Microb. Ecol. **70**: 215–232. doi:10.3354/ame01655

Georges, C., S. Monchy, S. Genitsaris, and U. Christaki. 2014. Protist community composition during early phytoplankton blooms in the naturally iron-fertilized Kerguelen area (Southern Ocean). Biogeosciences Discuss. **11**: 11179–11215. doi:10.5194/bgd-11-11179-2014

Giering, S. L. C., R. Sanders, R. S. Lampitt, and others. 2014. Reconciliation of the carbon budget in the ocean’s twilight zone. Nature **507**: 480–483. doi:10.1038/nature13123

Giering, S. L. C., R. Sanders, A. P. Martin, S. A. Henson, J. S. Riley, C. M. Marsay, and D. G. Johns. 2017. Particle flux in the oceans: Challenging the steady state assumption. Global Biogeochem. Cycles **31**: 159–171. doi:10.1002/2016GB005424

Giesecke, R., H. E. González, and U. Bathmann. 2010. The role of the chaetognath Sagitta gazellae in the vertical carbon flux of the Southern Ocean. Polar Biol. **33**: 293–304. doi:10.1007/s00300-009-0704-4

Gloeckler, K., C. A. Choy, C. C. S. Hannides, H. G. Close, E. Goetze, B. N. Popp, and J. C. Drazen. 2017. Stable isotope analysis of micronekton around Hawaii reveals suspended particles are an important nutritional source in the lower mesopelagic and upper bathypelagic zones. Limnol. Oceanogr. **0**. doi:10.1002/lno.10762

Godhe, A., M. E. Asplund, K. Härnström, V. Saravanan, A. Tyagi, and I. Karunasagar. 2008. Quantification of diatom and dinoflagellate biomasses in coastal marine seawater samples by real-time PCR. Appl. Environ. Microbiol. **74**: 7174–7182. doi:10.1128/AEM.01298-08

Gómez, F., D. Moreira, and P. López-García. 2009. Life cycle and molecular phylogeny of the dinoflagellates Chytriodinium and Dissodinium, ectoparasites of copepod eggs. Eur. J. Protistol. **45**: 260–270. doi:10.1016/j.ejop.2009.05.004

Gonçalves, V. N., A. B. M. Vaz, C. A. Rosa, and L. H. Rosa. 2012. Diversity and distribution of fungal communities in lakes of Antarctica. FEMS Microbiol. Ecol. **82**: 459–471. doi:10.1111/j.1574-6941.2012.01424.x

Gong, J., J. Dong, X. Liu, and R. Massana. 2013. Extremely High Copy Numbers and Polymorphisms of the rDNA Operon Estimated from Single Cell Analysis of Oligotrich and Peritrich Ciliates. Protist **164**: 369–379. doi:10.1016/j.protis.2012.11.006

Gowing, M. M., D. L. Garrison, H. B. Kunze, and C. J. Winchell. 2001. Biological components of Ross Sea short-term particle fluxes in the austral summer of 1995-1996. Deep. Res. Part I Oceanogr. Res. Pap. **48**: 2645–2671. doi:10.1016/S0967-0637(01)00034-6

Gowing, M. M., D. L. Garrison, K. F. Wishner, and C. Gelfman. 2003. Mesopelagic microplankton of the Arabian Sea. Deep. Res. Part I Oceanogr. Res. Pap. **50**: 1205–1234. doi:10.1016/S0967-0637(03)00130-4

Gowing, M. M., and M. W. Silver. 1985. Minipellets: A new and abundant size class of marine fecal pellets. J. Mar. Res. **43**: 395–418. doi:10.1357/002224085788438676

Grattepanche, J.-D., L. F. Santoferrara, G. B. McManus, and L. A. Katz. 2016. Unexpected biodiversity of ciliates in marine samples from below the photic zone. Mol. Ecol. **25**: 3987–4000. doi:10.1111/mec.13745

Grossart, H. P., S. Van den Wyngaert, M. Kagami, C. Wurzbacher, M. Cunliffe, and K. Rojas-Jimenez. 2019. Fungi in aquatic ecosystems. Nat. Rev. Microbiol. doi:10.1038/s41579-019-0175-8

Guillou, L., D. Bachar, S. Audic, and others. 2012. The Protist Ribosomal Reference database (PR2): a catalog of unicellular eukaryote Small Sub-Unit rRNA sequences with curated taxonomy. Nucleic Acids Res. **41**: D597–D604. doi:10.1093/nar/gks1160

Guillou, L., M. Viprey, A. Chambouvet, R. M. Welsh, A. R. Kirkham, R. Massana, D. J. Scanlan, and A. Z. Worden. 2008. Widespread occurrence and genetic diversity of marine parasitoids belonging to Syndiniales (Alveolata). Environ. Microbiol. **10**: 3349–3365. doi:10.1111/j.1462-2920.2008.01731.x

Gutierrez-Rodriguez, A., M. R. Stukel, A. Lopes dos Santos, T. Biard, R. Scharek, D. Vaulot, M. R. Landry, and F. Not. 2019. High contribution of Rhizaria (Radiolaria) to vertical export in the California Current Ecosystem revealed by DNA metabarcoding. ISME J. **13**: 964–976. doi:10.1038/s41396-018-0322-7

Gutiérrez, M. H., S. Pantoja, R. A. Quiñones, and R. R. González. 2010. First record of filamentous fungi in the coastal upwelling ecosystem off central Chile Primer registro de hongos filamentosos en el ecosistema de surgencia costero frente a Chile central. Gayana **74**: 66–73.

Gutiérrez, M. H., S. Pantoja, E. Tejos, and R. A. Quiñones. 2011. The role of fungi in processing marine organic matter in the upwelling ecosystem off Chile. Mar. Biol. **158**: 205–219. doi:10.1007/s00227-010-1552-z

Hadziavdic, K., K. Lekang, A. Lanzen, I. Jonassen, E. M. Thompson, and C. Troedsson. 2014. Characterization of the 18S rRNA Gene for Designing Universal Eukaryote Specific Primers C.R. Voolstra [ed.]. PLoS One **9**: e87624. doi:10.1371/journal.pone.0087624

Harada, A., S. Ohtsuka, and T. Horiguchi. 2007. Species of the Parasitic Genus Duboscquella are Members of the Enigmatic Marine Alveolate Group I. Protist **158**: 337–347. doi:10.1016/j.protis.2007.03.005

Head, M. J., R. Harland, and J. Matthiessen. 2001. Cold marine indicators of the late

Quaternary: The new dinoflagellate cyst genus Islandinium and related morphotypes. J. Quat. Sci. **16**: 621–636. doi:10.1002/jqs.657

Herndl, G. J., and T. Reinthaler. 2013. Microbial control of the dark end of the biological pump. Nat. Geosci. **6**: 718–724. doi:10.1038/ngeo1921

Hoffmann, L. J., I. Peeken, and K. Lochte. 2008. Iron, silicate, and light co-limitation of three Southern Ocean diatom species. Polar Biol. **31**: 1067–1080. doi:10.1007/s00300-008-0448-6

Hong, Y., W. O. Smith, and A.-M. White. 1997. Studies on Transparent Exopolymer Particles (Tep) Produced in the Ross Sea (Antarctica) and By Phaeocystis Antarctica (Prymnesiophyceae)1. J. Phycol. **33**: 368–376. doi:10.1111/j.0022-3646.1997.00368.x

Ishikawa, A., S. W. Wright, R. van den Enden, A. T. Davidson, and H. J. Marchant. 2002. Abundance , size structure and community composition of phytoplankton in the Southern Ocean in the austral summer 1999 / 2000. Polar Biosci. **15**: 11–26.

Jacques, G. 1983. Some ecophysiological aspects of the Antarctic phytoplankton. Polar Biol. **2**: 27–33. doi:10.1007/BF00258282

Jacques, G., and M. Panouse. 1991. Biomass and composition of size fractionated phytoplankton in the Weddell-Scotia Confluence area. Polar Biol. **11**: 315–328. doi:10.1007/BF00239024

Jensen, M. H., and N. Daugbjerg. 2009. MOLECULAR PHYLOGENY OF SELECTED SPECIES OF THE ORDER DINOPHYSIALES (DINOPHYCEAE)-TESTING THE HYPOTHESIS OF A DINOPHYSIOID RADIATION. J. Phycol. **45**: 1136–1152. doi:10.1111/j.1529-8817.2009.00741.x

Jeong, H. J., Y. Du Yoo, N. S. Kang, J. R. Rho, K. A. Seong, J. W. Park, G. S. Nam, and W. Yih. 2010. Ecology of Gymnodinium aureolum. I. Feeding in western Korean waters. Aquat. Microb. Ecol. **59**: 239–255. doi:10.3354/ame01394

Jiang, Y., E. J. Yang, J. O. Min, T. W. Kim, and S. H. Kang. 2015. Vertical variation of pelagic ciliate communities in the western Arctic Ocean. Deep. Res. Part II Top. Stud. Oceanogr. **120**: 103–113. doi:10.1016/j.dsr2.2014.09.005

Jin., X., N. Gruber, J. P. Dune, J. L. Sarmiento, and R. A. Armstrong. 2006. Diagnosing the contributions of phytoplankton functional groups to the production and export of particulate organic carbon, CaCO3, and opal from global nutrient and alkalinity distributions. Global Biogeochem. Cycles **20**: 1–17. doi:10.1029/2005GB002532

Kiørboe, T., and G. a. Jackson. 2001. Marine snow, organic solute plumes, and optimal chemosensory behavior of bacteria. Limnol. Oceanogr. **46**: 1309–1318. doi:10.4319/lo.2001.46.6.1309

Kirchman, D. L. 2008. Microbial Ecology of the Oceans, D.L. Kirchman [ed.]. John Wiley & Sons, Inc.

Klaas, C., and D. E. Archer. 2002. Association of sinking organic matter with various types of mineral ballast in the deep sea: Implications for the rain ratio. Global Biogeochem. Cycles **16**: 63-1-63–14. doi:10.1029/2001GB001765

Korb, R. E., M. J. Whitehouse, P. Ward, M. Gordon, H. J. Venables, and A. J. Poulton. 2012. Regional and seasonal differences in microplankton biomass, productivity, and structure across the Scotia Sea: Implications for the export of biogenic carbon. Deep. Res. Part II Top. Stud. Oceanogr. **59–60**: 67–77. doi:10.1016/j.dsr2.2011.06.006

Kwon, E. Y., F. Primeau, and J. L. Sarmiento. 2009. The impact of remineralization depth on the air–sea carbon balance. Nat. Geosci. **2**: 630–635. doi:10.1038/ngeo612

De La Rocha, C. L., and U. Passow. 2007. Factors influencing the sinking of POC and the efficiency of the biological carbon pump. Deep. Res. Part II Top. Stud. Oceanogr. **54**: 639–658. doi:10.1016/j.dsr2.2007.01.004

Lam, P. J., and O. Marchal. 2015. Insights into Particle Cycling from Thorium and Particle Data. Ann. Rev. Mar. Sci. **7**: 159–184. doi:10.1146/annurev-marine-010814-015623

Lam, P., M. M. Jensen, A. Kock, K. A. Lettmann, Y. Plancherel, G. Lavik, H. W. Bange, and M. M. M. Kuypers. 2011. Origin and fate of the secondary nitrite maximum in the Arabian Sea. Biogeosciences **8**: 1565–1577. doi:10.5194/bg-8-1565-2011

Lampitt, R. S., T. Noji, and B. von Bodungen. 1990. What happens to zooplankton faecal pellets? Implications for material flux. Mar. Biol. **104**: 15–23. doi:10.1007/BF01313152

Lampitt, R. S., I. Salter, and D. Johns. 2009. Radiolaria: Major exporters of organic carbon to the deep ocean. Global Biogeochem. Cycles **23**: 1–9. doi:10.1029/2008GB003221

Lampitt, R. S., K. F. Wishner, C. M. Turley, and M. V. Angel. 1993. Marine snow studies in the Northeast Atlantic Ocean: distribution, composition and role as a food source for migrating plankton. Mar. Biol. **116**: 689–702. doi:10.1007/BF00355486

Leblanc, K., B. Quéguiner, F. Diaz, and others. 2018. Nanoplanktonic diatoms are globally overlooked but play a role in spring blooms and carbon export. Nat. Commun. **9**: 1–12. doi:10.1038/s41467-018-03376-9

Legendre, L., and J. Le Fevre. 1995. Microbial food webs and the export of biogenic carbon in oceans. Aquat. Microb. Ecol. **9**: 69–77. doi:10.3354/ame009069

Legendre, L., and F. Rassoulzadegan. 1996. Food-web mediated export of biogenic carbon in oceans. Mar. Ecol. Prog. Ser. **145**: 179–193.

Lin, Y., N. Cassar, A. Marchetti, C. Moreno, H. Ducklow, and Z. Li. 2017. Specific eukaryotic plankton are good predictors of net community production in the Western Antarctic Peninsula. Sci. Rep. **7**: 1–11. doi:10.1038/s41598-017-14109-1

López-García, P., F. Rodríguez-Valera, C. Pedrós-Alió, and D. Moreira. 2001. Unexpected diversity of small eukaryotes in deep-sea Antarctic plankton. Nature **409**: 603–607. doi:10.1038/35054537

López-Pérez, M., A. Gonzaga, A.-B. Martin-Cuadrado, O. Onyshchenko, A. Ghavidel, R. Ghai, and F. Rodriguez-Valera. 2012. Genomes of surface isolates of Alteromonas macleodii: the life of a widespread marine opportunistic copiotroph. Sci. Rep. **2**: 696. doi:10.1038/srep00696

Marchant, H. J. 1985. Choanoflagellates in the Antarctic Marine Food Chain, p. 271–276. *In* Antarctic Nutrient Cycles and Food Webs. Springer Berlin Heidelberg.

Mari, X., U. Passow, C. Migon, A. B. Burd, and L. Legendre. 2017. Transparent exopolymer particles: Effects on carbon cycling in the ocean. Prog. Oceanogr. **151**: 13–37. doi:10.1016/j.pocean.2016.11.002

Martin, J. H., G. a. Knauer, D. M. Karl, and W. W. Broenkow. 1987. VERTEX: carbon cycling in the northeast Pacific. Deep Sea Res. Part A. Oceanogr. Res. Pap. **34**: 267–285. doi:10.1016/0198-0149(87)90086-0

Masella, A. P., A. K. Bartram, J. M. Truszkowski, D. G. Brown, and J. D. Neufeld. 2012. PANDAseq: PAired-eND Assembler for Illumina sequences. BMC Bioinformatics **13**: 31. doi:10.1186/1471-2105-13-31

Mayor, D. J., R. Sanders, S. L. C. Giering, and T. R. Anderson. 2014. Microbial gardening in the ocean's twilight zone: Detritivorous metazoans benefit from fragmenting, rather than ingesting, sinking detritus: Fragmentation of refractory detritus by zooplankton beneath the euphotic zone stimulates the harvestable productio. Bioessays 1132–1137. doi:10.1002/bies.201400100

McDonnell, A. M. P., P. J. Lam, C. H. Lamborg, and others. 2015. The oceanographic toolbox for the collection of sinking and suspended marine particles. Prog. Oceanogr. **133**: 17–31. doi:10.1016/j.pocean.2015.01.007

Medinger, R., V. Nolte, R. V. Pandey, S. Jost, B. Ottenwälder, C. Schlötterer, and J. Boenigk. 2010. Diversity in a hidden world: potential and limitation of next-generation sequencing for surveys of molecular diversity of eukaryotic microorganisms. Mol. Ecol. **19**: 32–40. doi:10.1111/j.1365-294X.2009.04478.x

Mestre, M., E. Borrull, Mm. Sala, and J. M. Gasol. 2017. Patterns of bacterial diversity in the marine planktonic particulate matter continuum. ISME J. 1–12. doi:10.1038/ismej.2016.166

Morgan-Smith, D., M. A. Clouse, G. J. Herndl, and A. B. Bochdansky. 2013. Diversity and distribution of microbial eukaryotes in the deep tropical and subtropical North Atlantic Ocean. Deep. Res. Part I Oceanogr. Res. Pap. **78**: 58–69. doi:10.1016/j.dsr.2013.04.010

Okolodkov, Y. B. 1999. Species range types of recent marine dinoflagellates recorded from the Arctic. Grana **38**: 162–169. doi:10.1080/00173139908559224

Orsi, W., Y. C. Song, S. Hallam, and V. Edgcomb. 2012. Effect of oxygen minimum zone formation on communities of marine protists. ISME J. **6**: 1586–1601. doi:10.1038/ismej.2012.7

Pahlow, M., U. Riebesell, and D. A. Wolf-Gladrow. 1997. Impact of cell shape and chain formation on nutrient acquisition by marine diatoms. Limnol. Oceanogr. **42**: 1660–1672. doi:10.4319/lo.1997.42.8.1660

Pakhomov, E. A., Y. Podeswa, B. P. V Hunt, and L. E. Kwong. 2018. Vertical distribution and active carbon transport by pelagic decapods in the North Pacific Subtropical Gyre. ICES J. Mar. Sci. doi:10.1093/icesjms/fsy134

Parris, D. J., S. Ganesh, V. P. Edgcomb, E. F. DeLong, and F. J. Stewart. 2014. Microbial eukaryote diversity in the marine oxygen minimum zone off northern Chile. Front. Microbiol. **5**: 1–11. doi:10.3389/fmicb.2014.00543

Passow, U., R. F. Shipe, A. Murray, D. K. Pak, M. A. Brzezinski, and A. L. Alldredge. 2001. The origin of transparent exopolymer particles (TEP) and their role in the sedimentation of particulate matter. Cont. Shelf Res. **21**: 327–346. doi:10.1016/S0278-4343(00)00101-1

Pernice, M. C., I. Forn, A. Gomes, and others. 2014. Global abundance of planktonic heterotrophic protists in the deep ocean. ISME J. **9**: 782–792. doi:10.1038/ismej.2014.168

Pernice, M. C., C. R. Giner, R. Logares, J. Perera-Bel, S. G. Acinas, C. M. Duarte, J. M. Gasol, and R. Massana. 2015. Large variability of bathypelagic microbial eukaryotic communities across the world's oceans. ISME J. 945–958. doi:10.1038/ismej.2015.170

Pernice, M. C., R. Logares, L. Guillou, and R. Massana. 2013. General Patterns of Diversity in Major Marine Microeukaryote Lineages. PLoS One **8**. doi:10.1371/journal.pone.0057170

Petrou, K., S. A. Kranz, S. Trimborn, C. S. Hassler, S. B. Ameijeiras, O. Sackett, P. J. Ralph, and A. T. Davidson. 2016. Southern Ocean phytoplankton physiology in a changing climate. J. Plant Physiol. **203**: 135–150. doi:10.1016/j.jplph.2016.05.004

Ploug, H., and H.-P. Grossart. 2000. Bacterial growth and grazing on diatom aggregates: Respiratory carbon turnover as a function of aggregate size and sinking velocity. Limnol. Oceanogr. **45**: 1467–1475. doi:10.4319/lo.2000.45.7.1467

Ploug, H., M. H. Iversen, and G. Fischer. 2008. Ballast, sinking velocity, and apparent diffusivity within marine snow and zooplankton fecal pellets: Implications for substrate turnover by attached bacteria. Limnol. Oceanogr. **53**: 1878–1886. doi:10.4319/lo.2008.53.5.1878

Pomeroy, L. R., and W. J. Wiebe. 1988. Energetics of microbial food webs. Hydrobiologia **159**: 7–18. doi:10.1007/BF00007363

Poulsen, L. K., and M. H. Iversen. 2008. Degradation of copepod fecal pellets: Key role of protozooplankton. Mar. Ecol. Prog. Ser. **367**: 1–13. doi:10.3354/meps07611

Poulton, R. E. K., M. J. Whitehouse, M. Gordon, P. Ward, and A.J. 2010. Summer microplankton community structure across the Scotia Sea: implications for biological carbon export. Biogeosciences **7**: 343–346.

Quast, C., E. Pruesse, P. Yilmaz, J. Gerken, T. Schweer, P. Yarza, J. Peplies, and F. O. Glöckner. 2013. The SILVA ribosomal RNA gene database project: Improved data processing and web-based tools. Nucleic Acids Res. **41**: 590–596. doi:10.1093/nar/gks1219

Rembauville, M., C. Manno, G. A. Tarling, S. Blain, and I. Salter. 2016. Strong contribution of diatom resting spores to deep-sea carbon transfer in naturally iron-fertilized waters downstream of South Georgia. Deep Sea Res. Part I Oceanogr. Res. Pap. **115**: 22–35.

doi:10.1016/j.dsr.2016.05.002

Riley, J. S., R. Sanders, C. Marsay, F. A. C. Le Moigne, E. P. Achterberg, and A. J. Poulton. 2012. The relative contribution of fast and slow sinking particles to ocean carbon export. Global Biogeochem. Cycles **26**: n/a-n/a. doi:10.1029/2011GB004085

Rodríguez-Marconi, S., R. De La Iglesia, B. Díez, C. A. Fonseca, E. Hajdu, N. Trefault, and N. Webster. 2015. Characterization of bacterial, archaeal and eukaryote symbionts from antarctic sponges reveals a high diversity at a three-domain level and a particular signature for this ecosystem. PLoS One **10**: 1–19. doi:10.1371/journal.pone.0138837

Rojas-Jimenez, K., C. Wurzbacher, E. C. Bourne, A. Chiuchiolo, J. C. Priscu, and H. P. Grossart. 2017. Early diverging lineages within Cryptomycota and Chytridiomycota dominate the fungal communities in ice-covered lakes of the McMurdo Dry Valleys, Antarctica. Sci. Rep. **7**: 1–11. doi:10.1038/s41598-017-15598-w

Safi, K. A., K. V. Robinson, J. A. Hall, J. Schwarz, and E. W. Maas. 2012. Ross Sea deep-ocean and epipelagic microzooplankton during the summer-autumn transition period. Aquat. Microb. Ecol. **67**: 123–137. doi:10.3354/ame01588

Sauvadet, A. L., A. Gobet, and L. Guillou. 2010. Comparative analysis between protist communities from the deep-sea pelagic ecosystem and specific deep hydrothermal habitats. Environ. Microbiol. **12**: 2946–2964. doi:10.1111/j.1462-2920.2010.02272.x

Schmoker, C., S. Hernández-León, and A. Calbet. 2013. Microzooplankton grazing in the oceans: Impacts, data variability, knowledge gaps and future directions. J. Plankton Res. **35**: 691–706. doi:10.1093/plankt/fbt023

Sedwick, P. N., and G. R. Ditullio. 1997. Regulation of algal blooms in Antarctic shelf waters by the release of iron from melting sea ice. Geophys. Res. Lett. **24**: 2515–2518.

doi:10.1029/97GL02596

Sherr, E. B., and B. F. Sherr. 2002. Significance of predation by protsts. Antonie Van Leeuwenhoek **81**: 293–308.

Sherr, E. B., and B. F. Sherr. 2007. Heterotrophic dinoflagellates: A significant component of microzooplankton biomass and major grazers of diatoms in the sea. Mar. Ecol. Prog. Ser. **352**: 187–197. doi:10.3354/meps07161

Silver, M. W., S. L. Coale, C. H. Pilskaln, and D. R. Steinberg. 1998. Giant aggregates: Importance as microbial centers and agents of material flux in the mesopelagic zone. Limnol. Oceanogr. **43**: 498–507. doi:10.4319/lo.1998.43.3.0498

Simon, M., H. P. Grossart, B. Schweitzer, and H. Ploug. 2002. Microbial ecology of organic aggregates in aquatic ecosystems. Aquat. Microb. Ecol. **28**: 175–211. doi:10.3354/ame028175

Skovgaard, A., S. A. Karpov, and L. Guillou. 2012. The parasitic dinoflagellates Blastodinium spp. Inhabiting the gut of marine, Planktonic copepods: Morphology, ecology, and unrecognized species diversity. Front. Microbiol. **3**: 1–22. doi:10.3389/fmicb.2012.00305

Skovgaard, A., R. Massana, V. Balagué, and E. Saiz. 2005. Phylogenetic position of the copepod-infesting parasite Syndinium turbo (Dinoflagellata, Syndinea). Protist **156**: 413–423. doi:10.1016/j.protis.2005.08.002

Smetacek, V., C. Klaas, S. Menden-Deuer, and T. A. Rynearson. 2002. Mesoscale distribution of dominant diatom species relative to the hydrographical field along the Antarctic Polar Front. Deep. Res. Part II Top. Stud. Oceanogr. **49**: 3835–3848. doi:10.1016/S0967-0645(02)00113-3

Smith, D. C., M. Simon, A. L. Alldredge, and F. Azam. 1992. Intense hydrolytic enzyme activity on marine aggregates and implications for rapid particle dissolution. Nature **359**: 139–142. doi:10.1038/359139a0

Smith, W. O., A. R. Shields, J. C. Dreyer, J. A. Peloquin, and V. Asper. 2011. Interannual variability in vertical export in the Ross Sea: Magnitude, composition, and environmental correlates. Deep. Res. Part I Oceanogr. Res. Pap. **58**: 147–159. doi:10.1016/j.dsr.2010.11.007

Stamieszkin, K., N. Poulton, and A. Pershing. 2017. Zooplankton grazing and egestion shifts particle size distribution in natural communities. Mar. Ecol. Prog. Ser. **575**: 43–56. doi:10.3354/meps12212

Steinberg, D. K., C. A. Carlson, N. R. Bates, S. A. Goldthwait, L. P. Madin, and A. F. Michaels. 2000. Zooplankton vertical migration and the active transport of dissolved organic and inorganic carbon in the Sargasso Sea. Deep. Res. Part I Oceanogr. Res. Pap. **47**: 137–158. doi:10.1016/S0967-0637(99)00052-7

Steinberg, D. K., and M. R. Landry. 2017. Zooplankton and the Ocean Carbon Cycle. Ann. Rev. Mar. Sci. **9**: 413–444. doi:10.1146/annurev-marine-010814-015924

Steinberg, D. K., B. a. S. Van Mooy, K. O. Buesseler, P. W. Boyd, T. Kobari, and D. M. Karl. 2008. Bacterial vs. zooplankton control of sinking particle flux in the ocean's twilight zone. Limnol. Oceanogr. **53**: 1327–1338. doi:10.4319/lo.2008.53.4.1327

Stoecker, D. K., P. J. Hansen, D. A. Caron, and A. Mitra. 2017. Mixotrophy in the Marine Plankton. Ann. Rev. Mar. Sci. **9**: 311–335. doi:10.1146/annurev-marine-010816-060617

Strom, S. L., R. Benner, S. Ziegler, and M. J. Dagg. 1997. Planktonic grazers are a potentially important source of marine dissolved organic carbon. Linmol. Ocean. **42**:

1364–1374.

Stukel, M. R., T. Biard, J. Krause, and M. D. Ohman. 2018. Large Phaeodaria in the twilight zone: Their role in the carbon cycle. Limnol. Oceanogr. **63**: 2579–2594. doi:10.1002/lno.10961

Suzuki, N., and Y. Aita. 2011. Radiolaria: achievements and unresolved issues: taxonomy and cytology. Plankt. Benthos Res. **6**: 69–91. doi:10.3800/pbr.6.69

Suzuki, N., and F. Not. 2015. Biology and Ecology of Radiolaria BT - Marine Protists: Diversity and Dynamics, p. 179–222. *In* S. Ohtsuka, T. Suzaki, T. Horiguchi, N. Suzuki, and F. Not [eds.]. Springer Japan.

Tanaka, T., and F. Rassoulzadegan. 2002. Full-depth profile (0–2000m) of bacteria, heterotrophic nanoflagellates and ciliates in the NW Mediterranean Sea: Vertical partitioning of microbial trophic structures. Deep Sea Res. Part II Top. Stud. Oceanogr. **49**: 2093–2107. doi:10.1016/S0967-0645(02)00029-2

Taylor, G. T., and C. W. Sullivan. 2008. Vitamin B12and cobalt cycling among diatoms and bacteria in Antarctic sea ice microbial communities. Limnol. Oceanogr. **53**: 1862–1877. doi:10.4319/lo.2008.53.5.1862

Taylor, J. D., and M. Cunliffe. 2016. Multi-year assessment of coastal planktonic fungi reveals environmental drivers of diversity and abundance. ISME J. **10**: 1–11. doi:10.1038/ismej.2016.24

Thomsen, H. a., K. R. Buck, P. a. Bolt, and D. L. Garrison. 1991. Fine structure and biology of Cryothecomonas gen. nov. (Protista incertae sedis) from the ice biota. Can. J. Zool. **69**: 1048–1070. doi:10.1139/z91-150

Thomsen, P. F., J. Kielgast, L. L. Iversen, P. R. Møller, M. Rasmussen, and E. Willerslev. 2012. Detection of a Diverse Marine Fish Fauna Using Environmental DNA from Seawater Samples. PLoS One **7**: 1–9. doi:10.1371/journal.pone.0041732

Tréguer, P., C. Bowler, B. Moriceau, and others. 2018. Influence of diatom diversity on the ocean biological carbon pump. Nat. Geosci. **11**: 27–37. doi:10.1038/s41561-017-0028-x

Turner, J. T. 2015. Zooplankton fecal pellets, marine snow, phytodetritus and the ocean's biological pump. Prog. Oceanogr. **130**: 205–248. doi:10.1016/j.pocean.2014.08.005

de Vargas, C., S. Audic, N. Henry, and others. 2015. Ocean plankton. Eukaryotic plankton diversity in the sunlit ocean. Science **348**: 1261605. doi:10.1126/science.1261605

Verdugo, P., A. L. Alldredge, F. Azam, D. L. Kirchman, U. Passow, and P. H. Santschi. 2004. The oceanic gel phase: A bridge in the DOM-POM continuum. Mar. Chem. **92**: 67–85. doi:10.1029/2002GL016046

Viprey, M., L. Guillou, M. Ferréol, and D. Vaulot. 2008. Wide genetic diversity of picoplanktonic green algae (Chloroplastida) in the Mediterranean Sea uncovered by a phylum-biased PCR approach. Environ. Microbiol. **10**: 1804–1822. doi:10.1111/j.1462-2920.2008.01602.x

Williams, R. A. J., H. L. Owens, J. Clamp, A. T. Peterson, A. Warren, and M. Martín-Cereceda. 2018. Endemicity and climatic niche differentiation in three marine ciliated protists. Limnol. Oceanogr. **63**: 2727–2736. doi:10.1002/lno.11003

Wilson, S. E., D. K. Steinberg, and K. O. Buesseler. 2008. Changes in fecal pellet characteristics with depth as indicators of zooplankton repackaging of particles in the mesopelagic zone of the subtropical and subarctic North Pacific Ocean. Deep. Res. Part II Top. Stud. Oceanogr. **55**: 1636–1647. doi:10.1016/j.dsr2.2008.04.019

Worden, a. Z., M. J. Follows, S. J. Giovannoni, S. Wilken, a. E. Zimmerman, and P. J. Keeling. 2015. Rethinking the marine carbon cycle: Factoring in the multifarious lifestyles of microbes. Science (80-. ). **347**: 1257594–1257594. doi:10.1126/science.1257594

Yang, E. J., J.-H. Hyun, D. Kim, J. Park, S.-H. Kang, H. C. Shin, and S. Lee. 2012. Mesoscale distribution of protozooplankton communities and their herbivory in the western Scotia Sea of the Southern Ocean during the austral spring. J. Exp. Mar. Bio. Ecol. **428**: 5–15. doi:10.1016/j.jembe.2012.05.018

Yebra, L., I. Herrera, J. M. Mercado, and others. 2018. Zooplankton production and carbon export flux in the western Alboran Sea gyre (SW Mediterranean). Prog. Oceanogr. **167**: 64–77. doi:10.1016/j.pocean.2018.07.009

Zhu, F., R. Massana, F. Not, D. Marie, and D. Vaulot. 2005. Mapping of picoeucaryotes in marine ecosystems with quantitative PCR of the 18S rRNA gene. FEMS Microbiol. Ecol. **52**: 79–92. doi:10.1016/j.femsec.2004.10.006

Zoccarato, L., A. Pallavicini, F. Cerino, S. Fonda Umani, and M. Celussi. 2016. Water mass dynamics shape Ross Sea protist communities in mesopelagic and bathypelagic layers. Prog. Oceanogr. **149**: 16–26. doi:10.1016/j.pocean.2016.10.003

## Acknowledgments

We sincerely thank the officers and crew of the *RRS James Clark Ross* for their logistical and technical support during the JR304 cruise, Anna Belcher (British Antarctic Survey) for sharing particulate organic carbon data, and Dr Alison Baylay at the Environmental Genomics Facility (University of Southampton) for her assistance on next-generation sequencing. Funding support came from University of Southampton (Start-up Grant for PL) and the Natural Environment Research Council. We thank the reviewers for contributing to enhance the quality of this manuscript.

**Figures and table legends**

**Figure 1. Location of sampling sites on a map of surface particulate organic carbon.** The map was constructed on Ocean Data View using data from NASA Ocean Color 9 km resolution level 3 browser. The surface particulate organic carbon data was corrected by D. Stramski 2007 method (version 443/555) and correspond to a 32-day composition (17/11/2014-18/12/2014).

**Figure 2. Canonical correspondence analysis of OTU composition.** The CCA was calculated on the total rarefied dataset. The significance of environmental parameters (oxygen, fluorescence, POC concentrations and temperature) was tested with a PERMANOVA ($p < 0.05$) (Table S3). Significant environmental parameters are displayed and their respective arrow length is proportional to the variability in community structure explain. ML = mixed layer, UM = upper-mesopelagic; SS0.22 = suspended particles 0.22 – 10 µm; SS10 = suspended particles 10 – 100 µm; SS100 = suspended particles ≥ 100 µm; (SS100), SK10 = sinking particles ≥ 10 µm.

**Figure 3. Total eukaryotic community composition.** Pie charts were constructed with the relative abundance of selected taxa in the total rarefied dataset. Sequences were subcategorised into metazoan (copepod, soft-tissue animal and other), phytoplankton (diatom, prymnesiophyte and other), other protists and fungi (dinoflagellates, *Syndinales*, ciliates, *Rhizaria* and other) and unassigned sequences. SS0.22 = suspended particles 0.22 – 10 µm; SS10 = suspended particles 10 – 100 µm; SS100 = suspended particles ≥ 100 µm; (SS100), SK10 = sinking particles ≥ 10 µm.

**Figure 4. Taxonomic composition of phytoplankton and metazoan.** Panel A displays the relative abundance of the 9 most abundant phytoplankton orders, and panel the relative

abundance of the 9 most abundant metazoan subclasses. Presented data was normalised to the considered taxonomic group (i.e., phytoplankton and metazoan). SS0.22 = suspended particles 0.22 – 10 µm; SS10 = suspended particles 10 – 100 µm; SS100 = suspended particles ≥ 100 µm; (SS100), SK10 = sinking particles ≥ 10 µm; ML = mixed layer, UM = upper-mesopelagic; Haptoph. = Haptophyte.

**Figure 5. Enrichment of phytoplankton taxonomic families in sinking and suspended particles.** Enrichments were calculated using Equation 1 on the phytoplankton normalised dataset. Negative values (in green) indicate an enrichment within sinking particles in the mixed layer and positive values (in red) indicate an enrichment within the compared sample in the upper-mesopelagic.

**Figure 6. Heterotrophic protists and fungi communities in sinking and suspended particles in the upper-mesopelagic.** Presented data was normalised to the considered taxonomic group (i.e., dinoflagellates, choanoflagellates, *Syndiniales*, ciliates, rhizarians and fungi), and transformed on using the formula $\log_2(x) + 1$ when $x > 0$ and where x is the relative abundance normalised within each taxonomic group considered. SS0.22 = suspended particles 0.22 – 10 µm; SS10 = suspended particles 10 – 100 µm; SS100 = suspended particles ≥ 100 µm; (SS100), SK10 = sinking particles ≥ 10 µm; OTU = % OTUs shared; seq = % affiliated sequences; Choano. = Choanoflagellata.

**Table 1. Percentages of OTUs and affiliated sequences shared between particle-fractions.** The proportions of phytoplankton and metazoan shared OTUs were calculated on the rarefied dataset. ML = mixed layer, UM = upper-mesopelagic; SS0.22 = suspended particles 0.22 – 10 µm; SS10 = suspended particles 10 – 100 µm; SS100 = suspended particles ≥ 100 µm; (SS100), SK10 = sinking particles ≥ 10 µm; OTU = % OTUs shared; seq = % affiliated sequences.

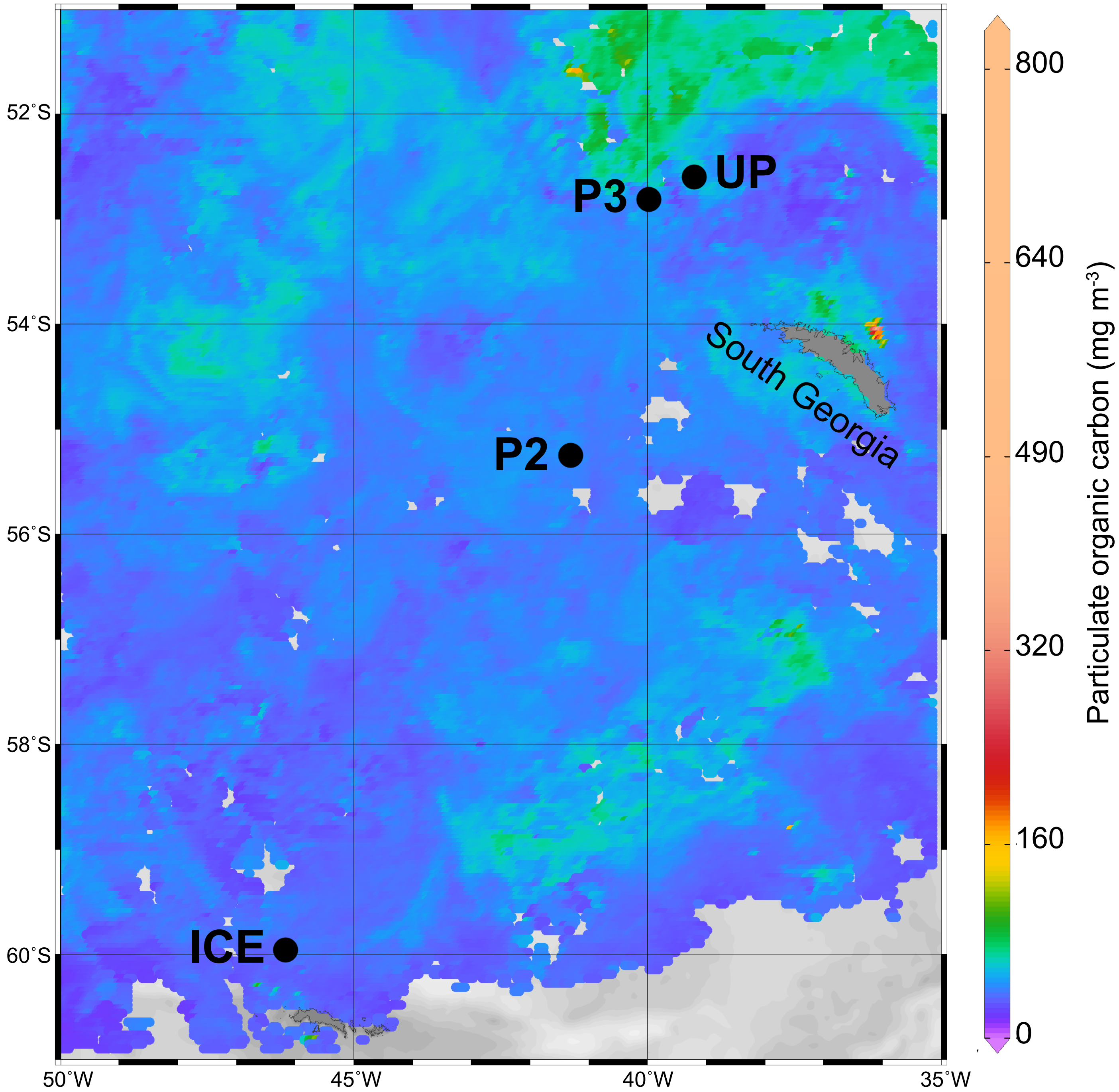

52°S
54°S
56°S
58°S
60°S
50°W
45°W
40°W
35°W
UP
P3
P2
ICE
South Georgia
800
640
490
320
160
0
Particulate organic carbon (mg m-3)


**Figure 1**

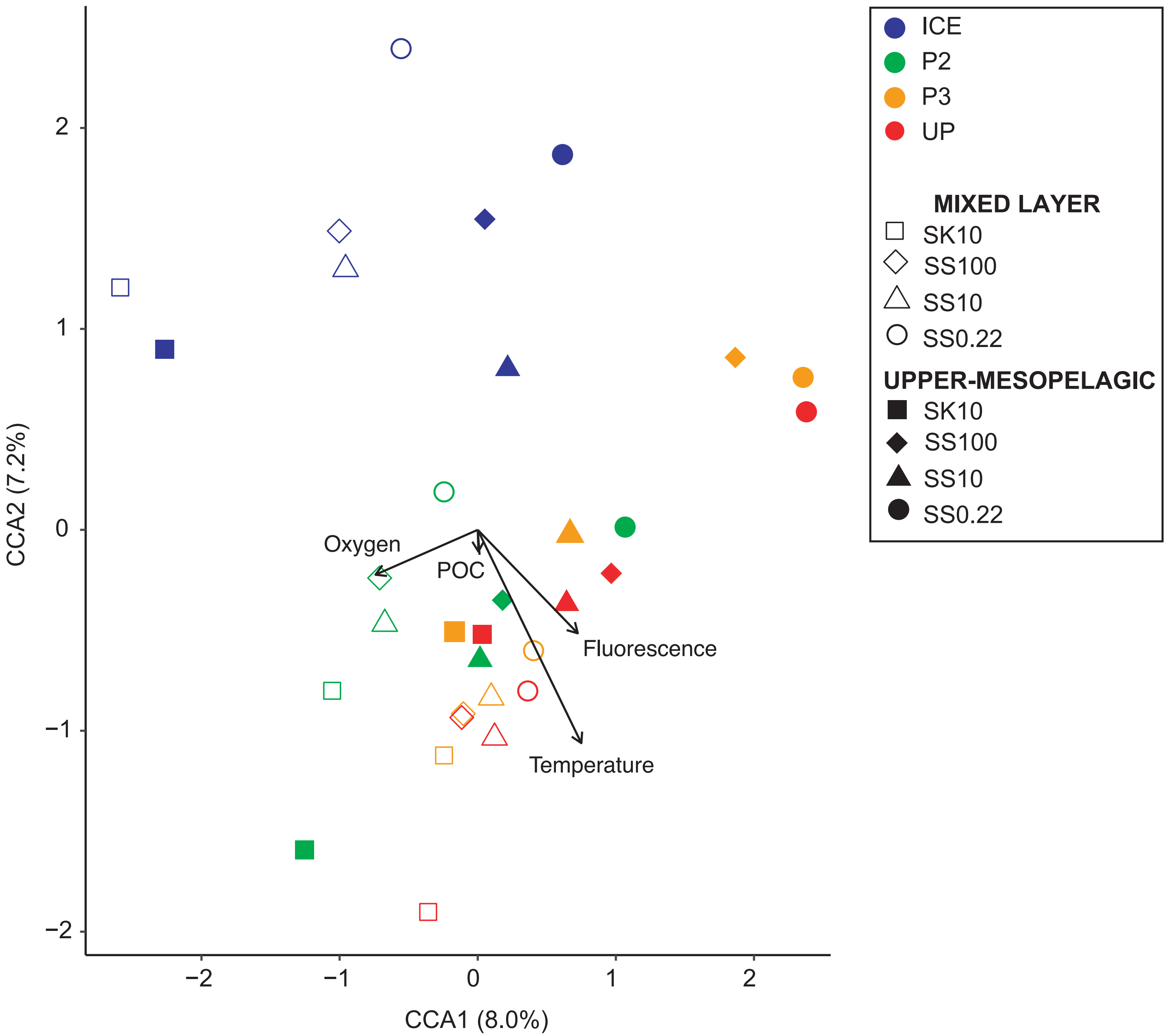

ICE
P2
P3
UP
MIXED LAYER
SK10
SS100
SS10
SS0.22
UPPER-MESOPELAGIC
SK10
SS100
SS10
SS0.22
Oxygen
POC
Fluorescence
Temperature
CCA1 (8.0%)
CCA2 (7.2%)
−2
−1
0
1
2


Figure 2

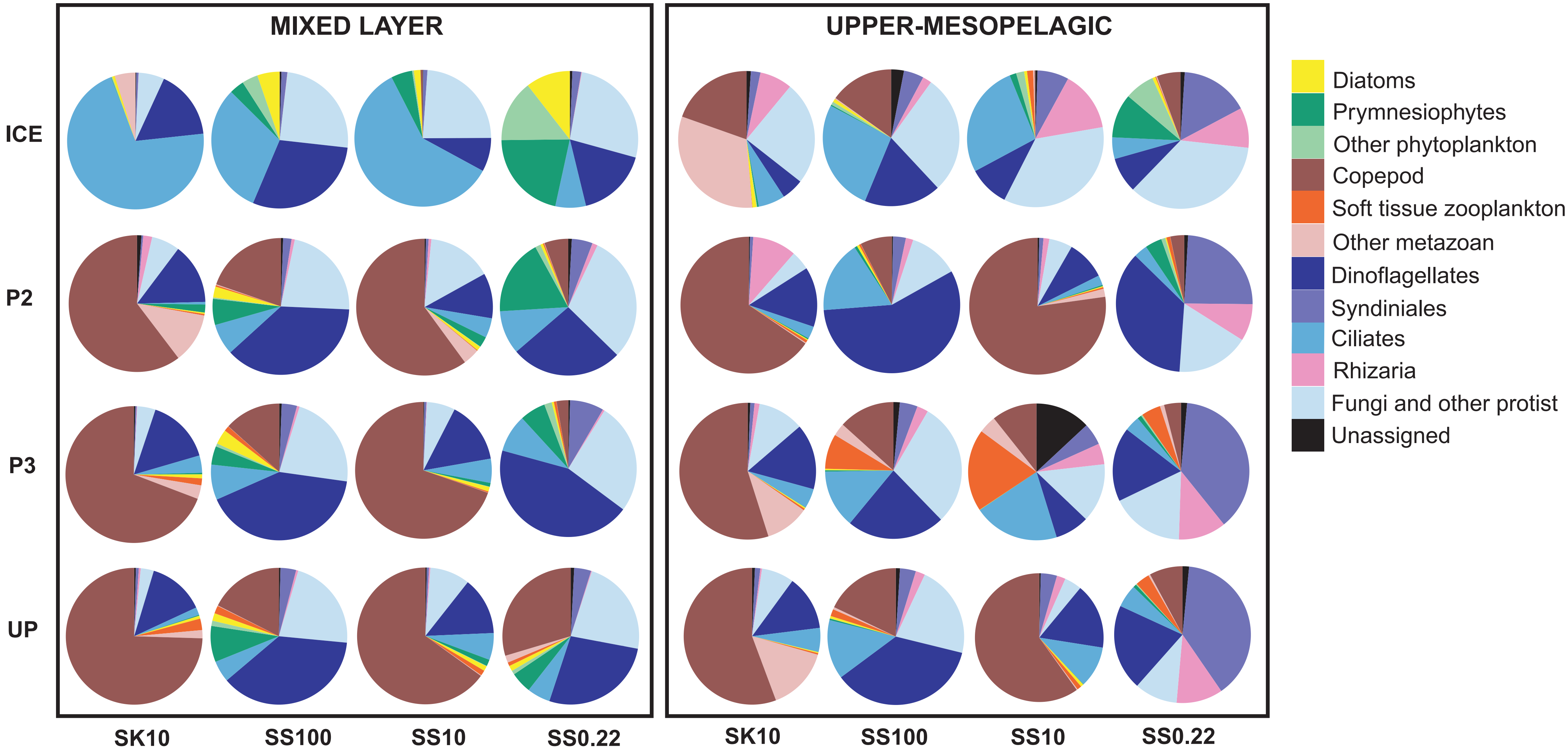
MIXED LAYER
UPPER-MESOPELAGIC
ICE
P2
P3
UP
SK10
SS100
SS10
SS0.22
Diatoms
Prymnesiophytes
Other phytoplankton
Copepod
Soft tissue zooplankton
Other metazoan
Dinoflagellates
Syndiniales
Ciliates
Rhizaria
Fungi and other protist
Unassigned

Figure 3

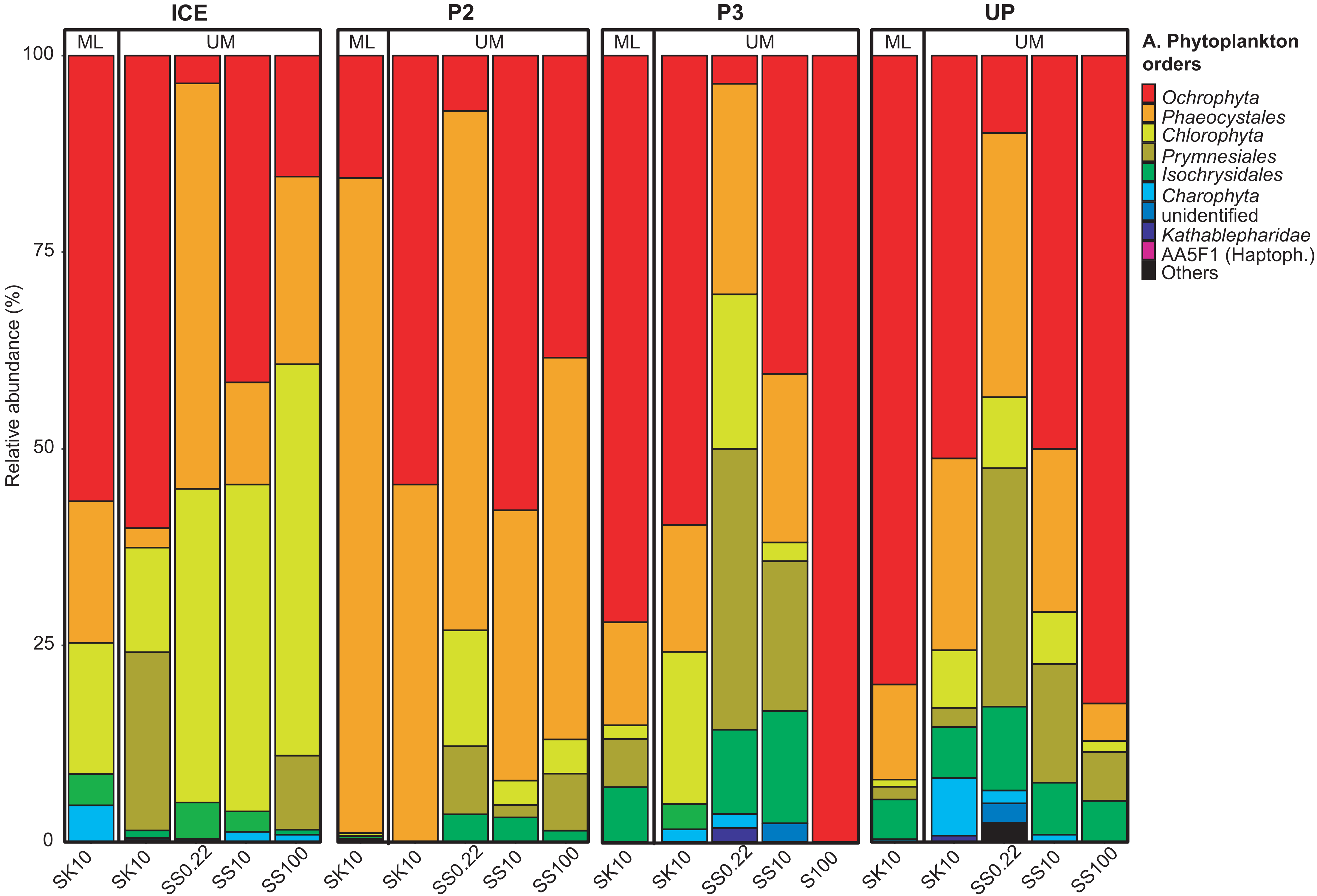
ICE
P2
P3
UP
ML
UM
Relative abundance (%)
100
75
50
25
0
SK10
SS0.22
SS10
SS100
S100
A. Phytoplankton orders
Ochrophyta
Phaeocystales
Chlorophyta
Prymnesiales
Isochrysidales
Charophyta
unidentified
Kathablepharidae
AA5F1 (Haptoph.)
Others

Figure 4-A

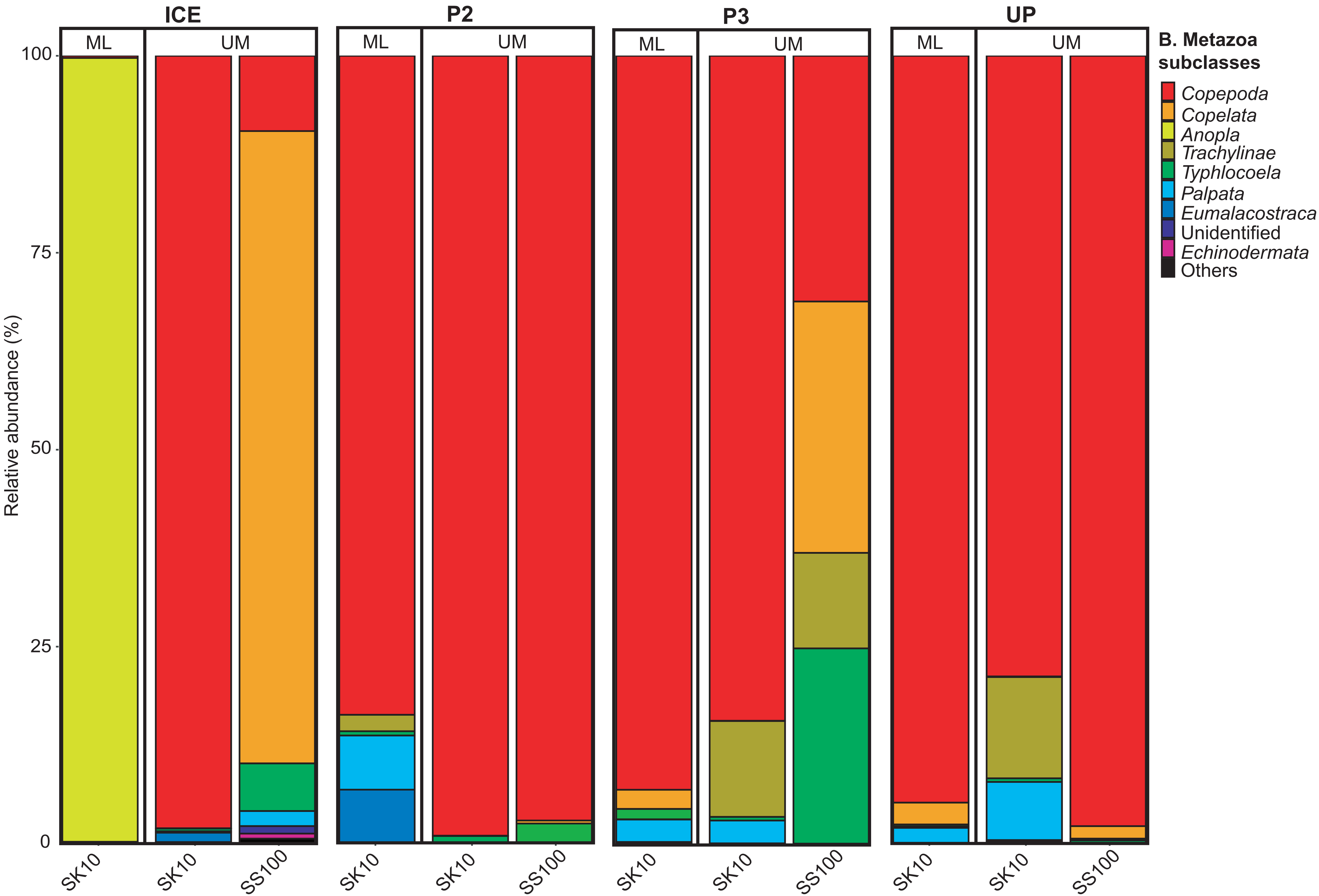
ICE
P2
P3
UP
ML
UM
Relative abundance (%)
0
25
50
75
100
SK10
SS100
B. Metazoa subclasses
Copepoda
Copelata
Anopla
Trachylinae
Typhlocoela
Palpata
Eumalacostraca
Unidentified
Echinodermata
Others

Figure 4-B

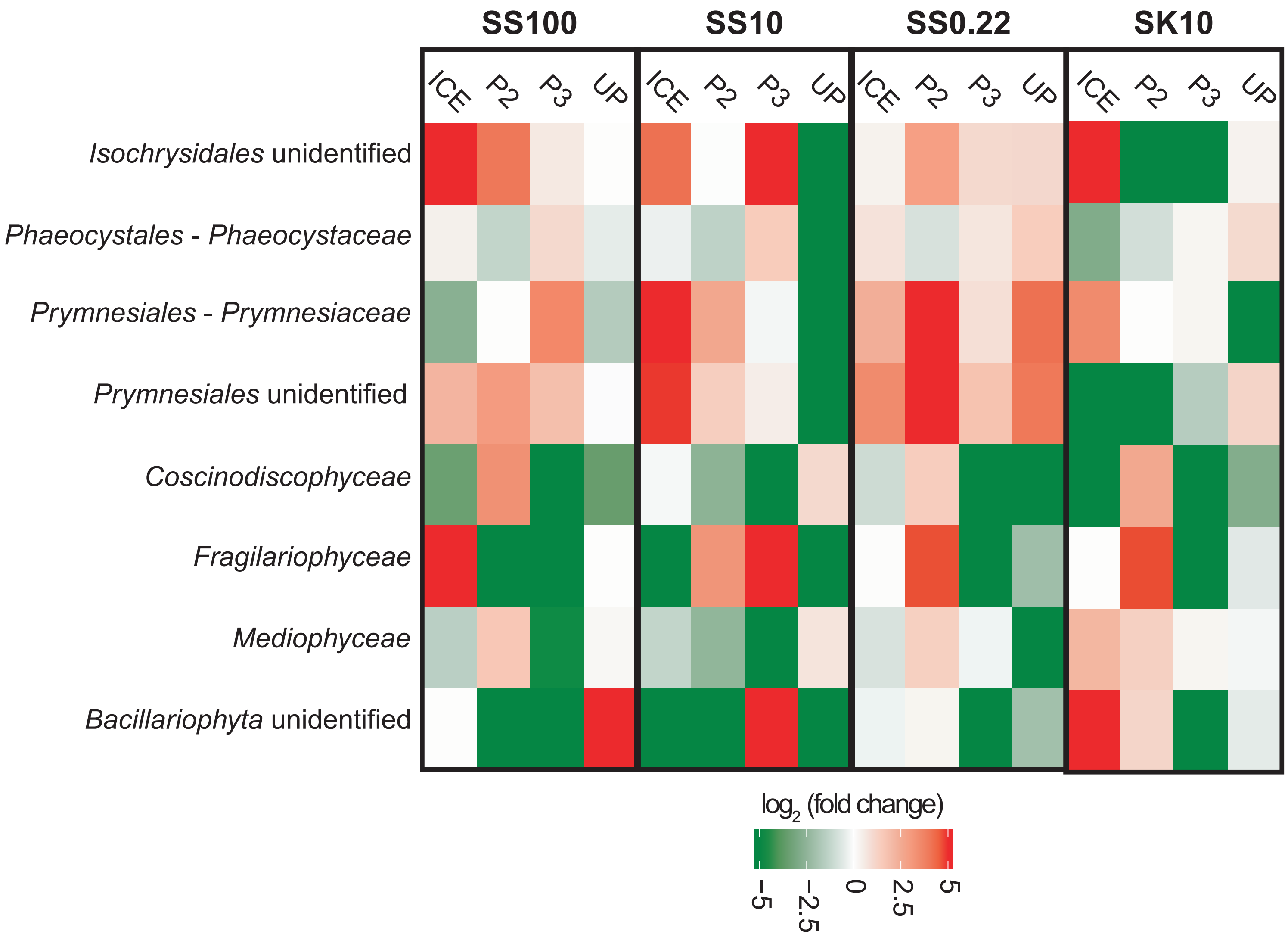

SS100
SS10
SS0.22
SK10
ICE
P2
P3
UP
Isochrysidales unidentified
Phaeocystales - Phaeocystaceae
Prymnesiales - Prymnesiaceae
Prymnesiales unidentified
Coscinodiscophyceae
Fragilariophyceae
Mediophyceae
Bacillariophyta unidentified
log2 (fold change)
−5
−2.5
0
2.5
5


Figure 5

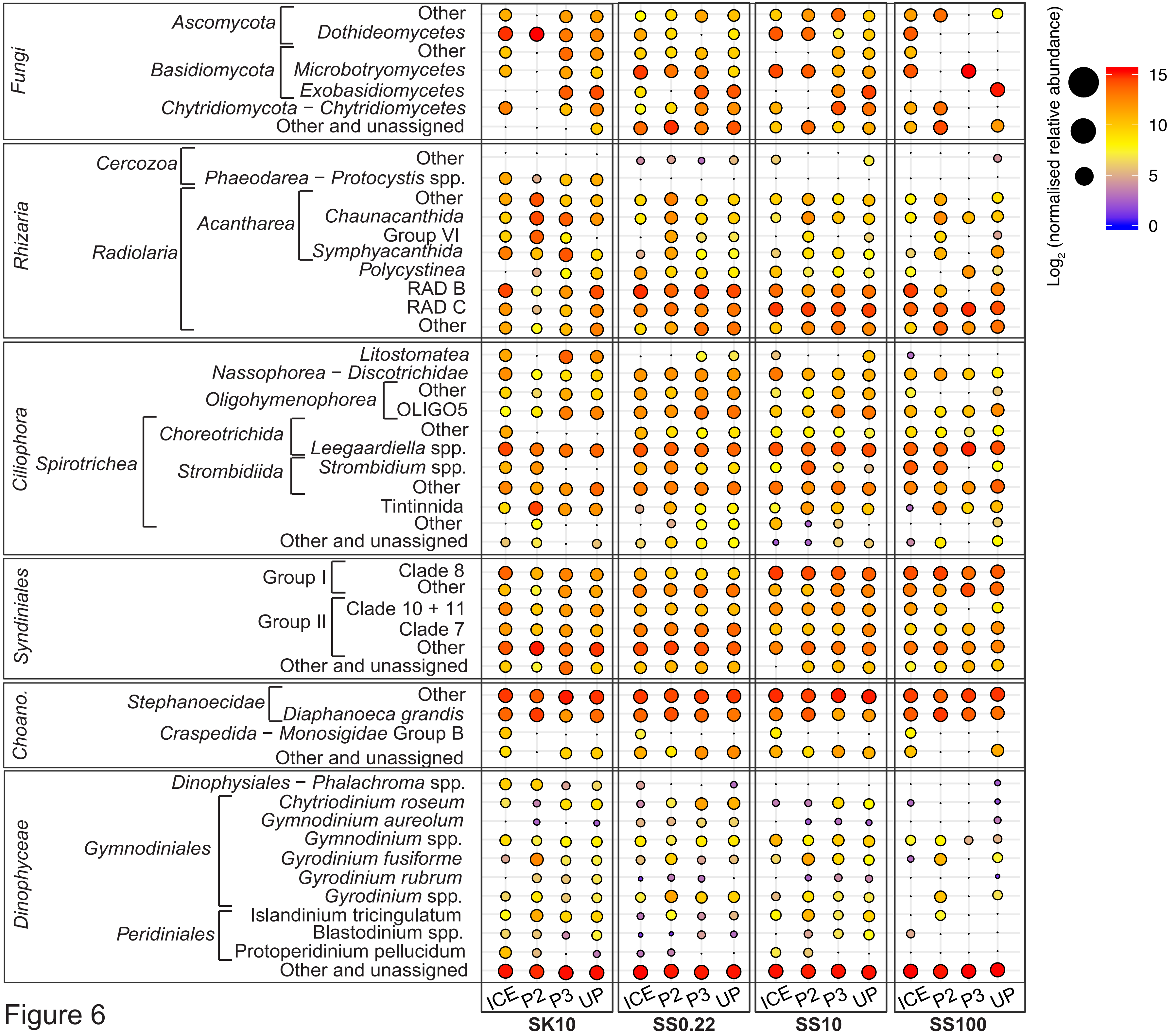
Fungi
Ascomycota
Other
Dothideomycetes
Basidiomycota
Other
Microbotryomycetes
Exobasidiomycetes
Chytridiomycota – Chytridiomycetes
Other and unassigned
Rhizaria
Cercozoa
Other
Phaeodarea – Protocystis spp.
Radiolaria
Acantharea
Other
Chaunacanthida
Group VI
Symphyacanthida
Polycystinea
RAD B
RAD C
Other
Ciliophora
Litostomatea
Nassophorea – Discotrichidae
Oligohymenophorea
Other
OLIGO5
Spirotrichea
Choreotrichida
Other
Leegaardiella spp.
Strombidiida
Strombidium spp.
Other
Tintinnida
Other
Other and unassigned
Syndiniales
Group I
Clade 8
Other
Group II
Clade 10 + 11
Clade 7
Other
Other and unassigned
Choano.
Stephanoecidae
Other
Diaphanoeca grandis
Craspedida – Monosigidae Group B
Other and unassigned
Dinophyceae
Dinophysiales – Phalachroma spp.
Gymnodiniales
Chytriodinium roseum
Gymnodinium aureolum
Gymnodinium spp.
Gyrodinium fusiforme
Gyrodinium rubrum
Gyrodinium spp.
Peridiniales
Islandinium tricingulatum
Blastodinium spp.
Protoperidinium pellucidum
Other and unassigned
ICE P2 P3 UP
SK10
ICE P2 P3 UP
SS0.22
ICE P2 P3 UP
SS10
ICE P2 P3 UP
SS100
Log2 (normalised relative abundance)
0
5
10
15

Figure 6

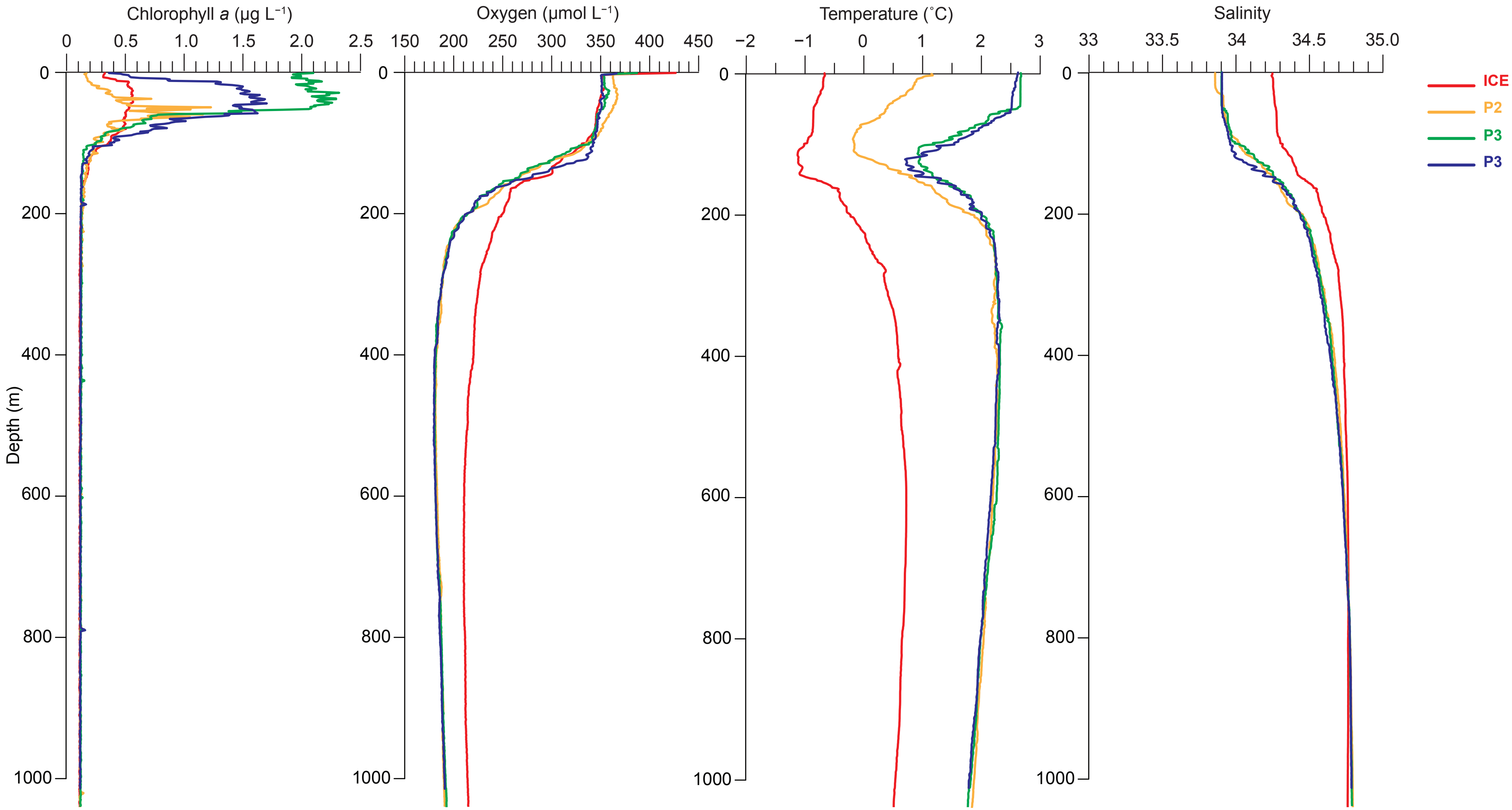


**Fig. S1 – Environmental parameters profiles.** Temperature, oxygen concentration and chlorophyll *a* concentration based on fluorescence measurements were obtained with a conductivity-temperature-depth device (CTD Seabird 9Plus with SBE32 carousel).

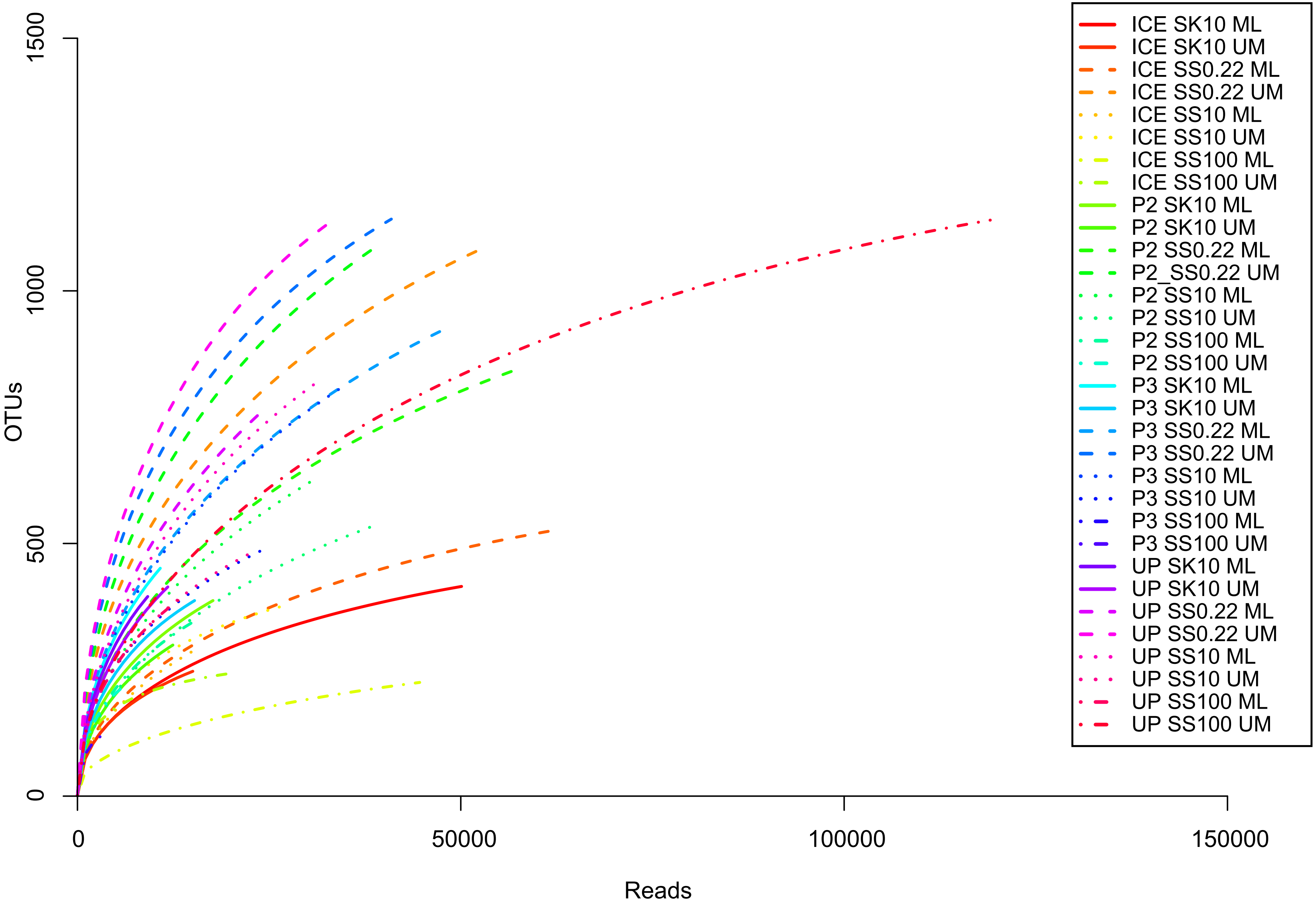


**Fig. S2 – Rarefaction curves.** ML = mixed layer, UM = upper-mesopelagic; SS0.22 = suspended particles 0.22 – 10 µm; SS10 = suspended particles 10 – 100 µm; SS100 = suspended particles ≥ 100 µm; (SS100), SK10 = sinking particles ≥ 10 µm.

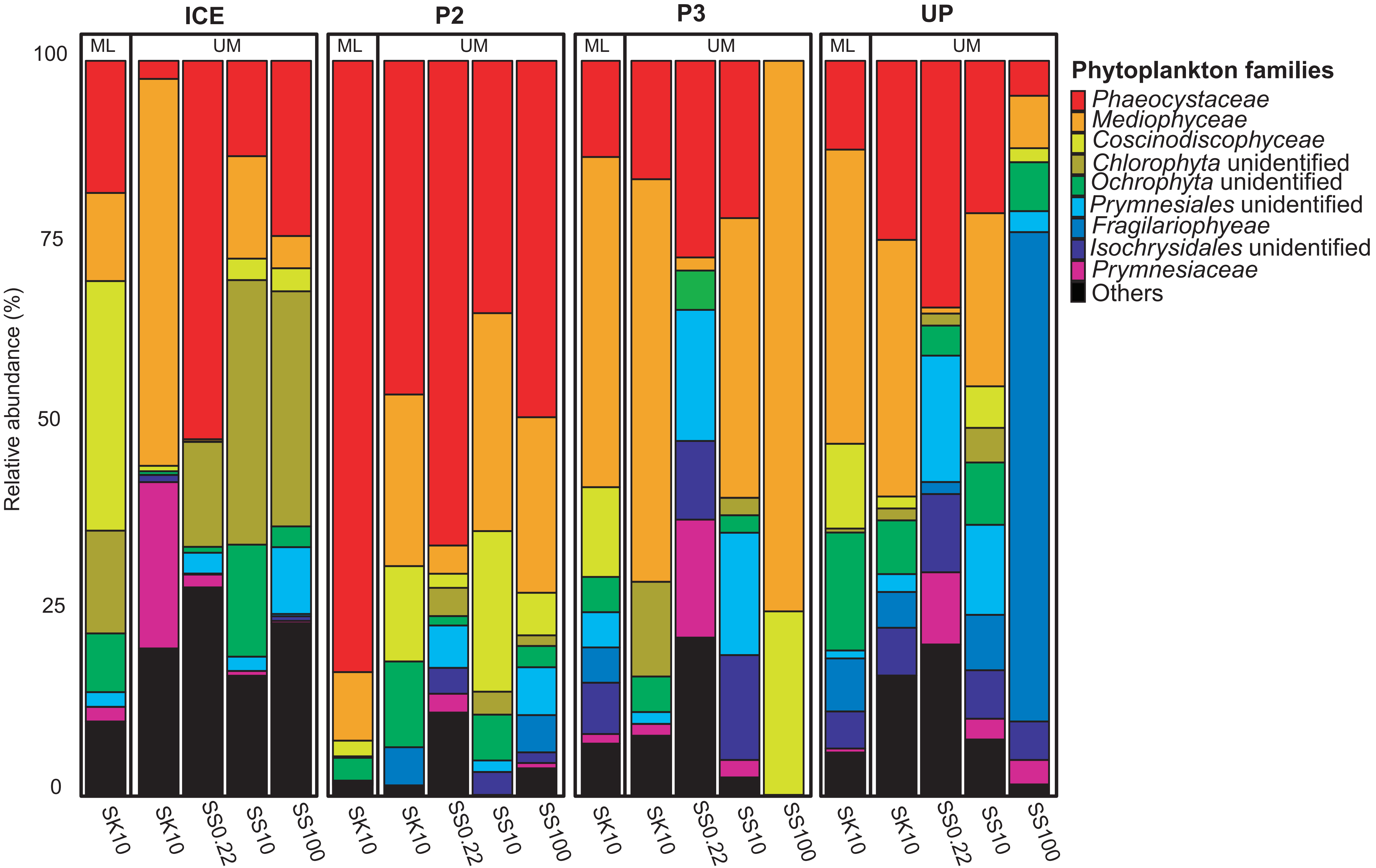


**Fig. S3 – Taxomomic family composition of phytoplankton communities.** Relative abundance of the 9 most represented phytoplankton families. ML = mixed layer, UM = upper-mesopelagic; SS0.22 = suspended particles 0.22 – 10 µm; SS10 = suspended particles 10 – 100 µm; SS100 = suspended particles ≥ 100 µm; (SS100), SK10 = sinking particles ≥ 10 µm.

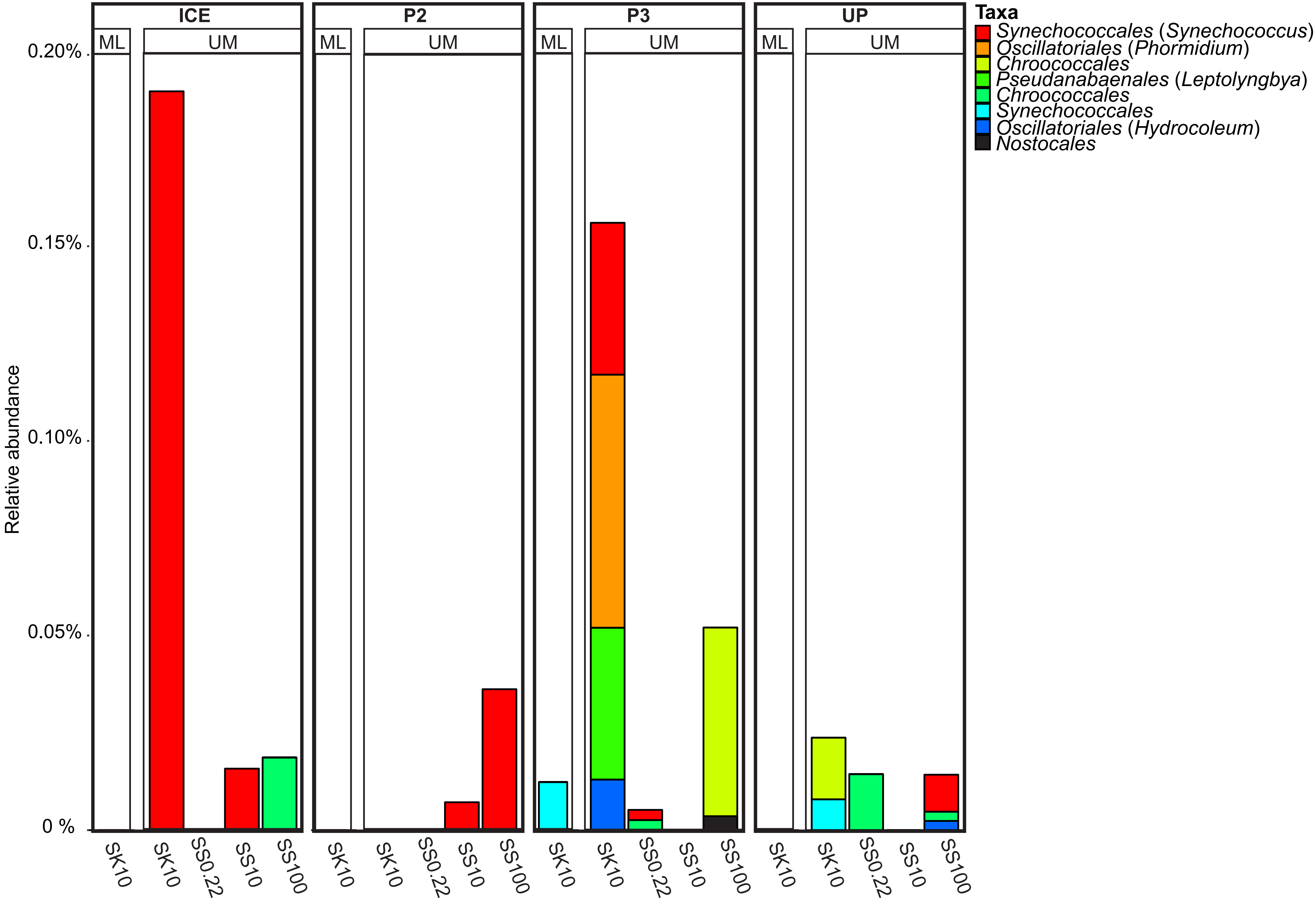


**Fig. S4-A – Taxomomic composition of cyanobacteria.** ML = mixed layer, UM = upper-mesopelagic; SS0.22 = suspended particles 0.22 – 10 µm; SS10 = suspended particles 10 – 100 µm; SS100 = suspended particles ≥ 100 µm; (SS100), SK10 = sinking particles ≥ 10 µm.

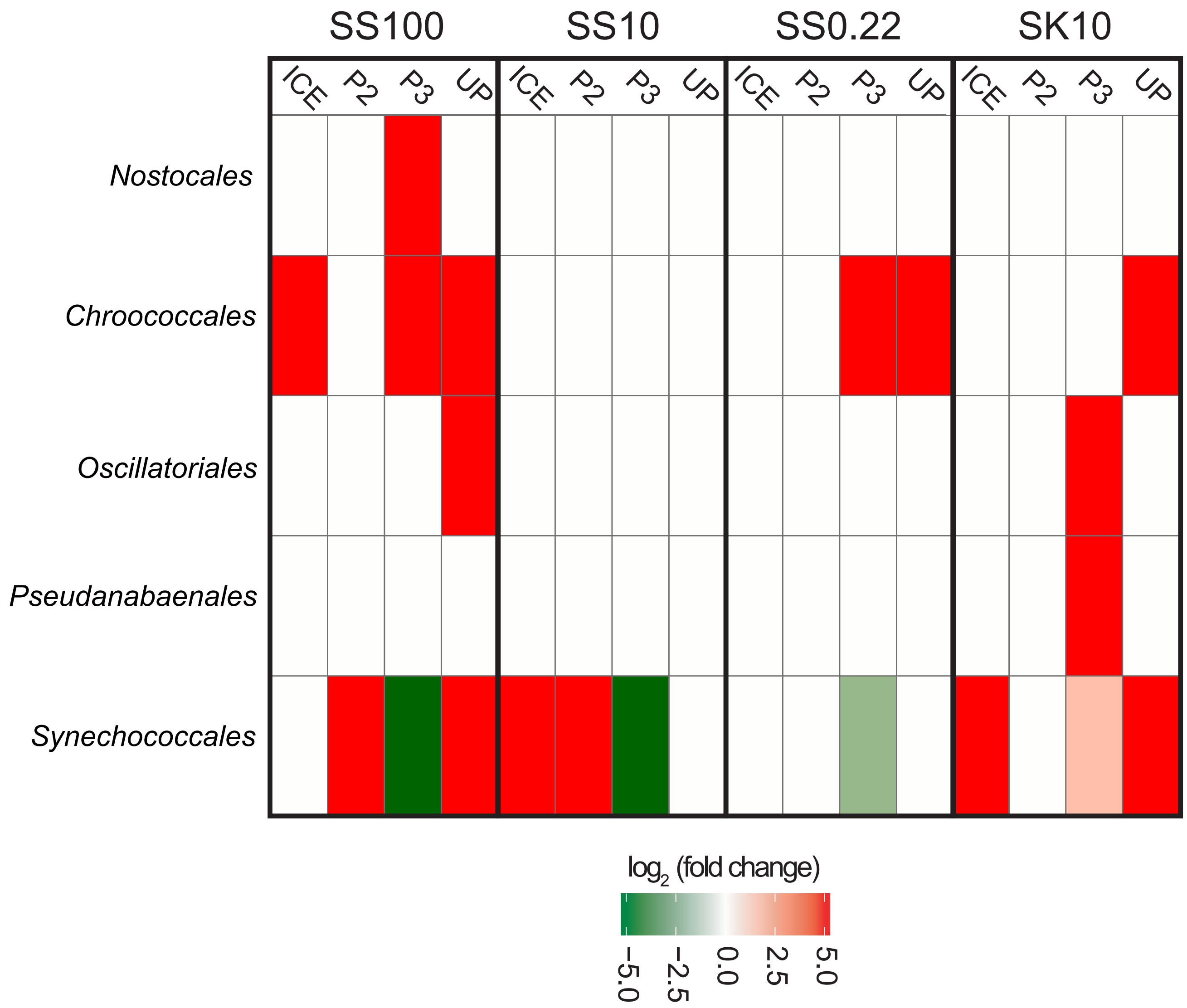


**Fig. S4-B – Enrichment of cyanobacterial taxa in sinking and suspended particles.** Enrichments were calculated using Equation 1 on the relative abundance normalised to the entired 16S rRNA gene amplicon sequencing dataset. Negative values (in green) indicate an enrichment within sinking particles in the mixed layer and positive values (in red) indicated an enrichment within the compared sample in the upper-mesopelagic. SS0.22 = suspended particles 0.22 – 10 µm; SS10 = suspended particles 10 – 100 µm; SS100 = suspended particles ≥ 100 µm; (SS100), SK10 = sinking particles ≥ 10 µm.

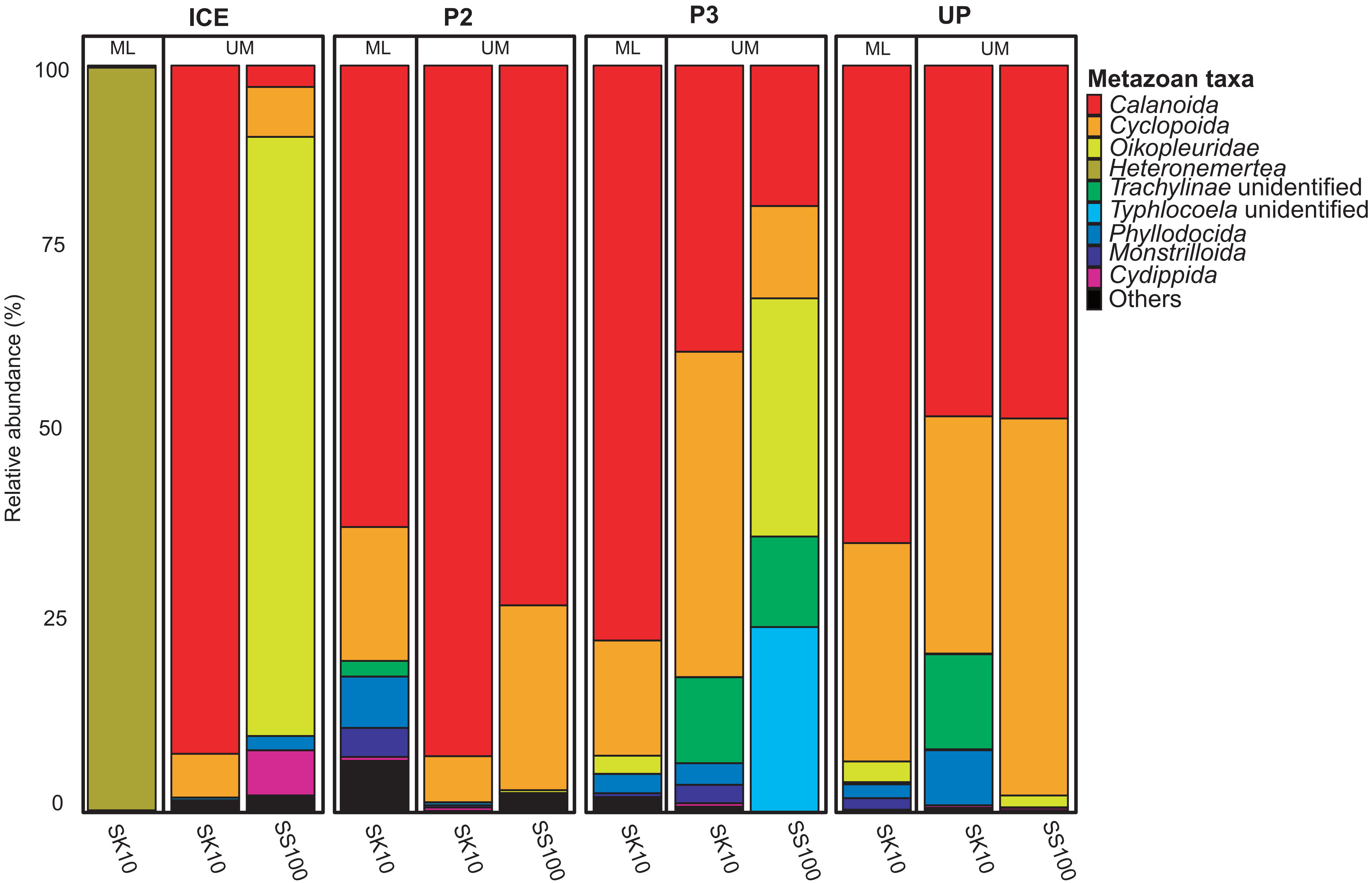


**Fig. S5 – Taxomomic composition of metazoan communities at lower taxonomic level.** Relative abundance of the 9 most represented metazoan taxa (at the highest taxonomic resolution offered by the Silva database). ML = mixed layer, UM = upper-mesopelagic; SS0.22 = suspended particles 0.22 – 10 µm; SS10 = suspended particles 10 – 100 µm; SS100 = suspended particles ≥ 100 µm; (SS100), SK10 = sinking particles ≥ 10 µm.

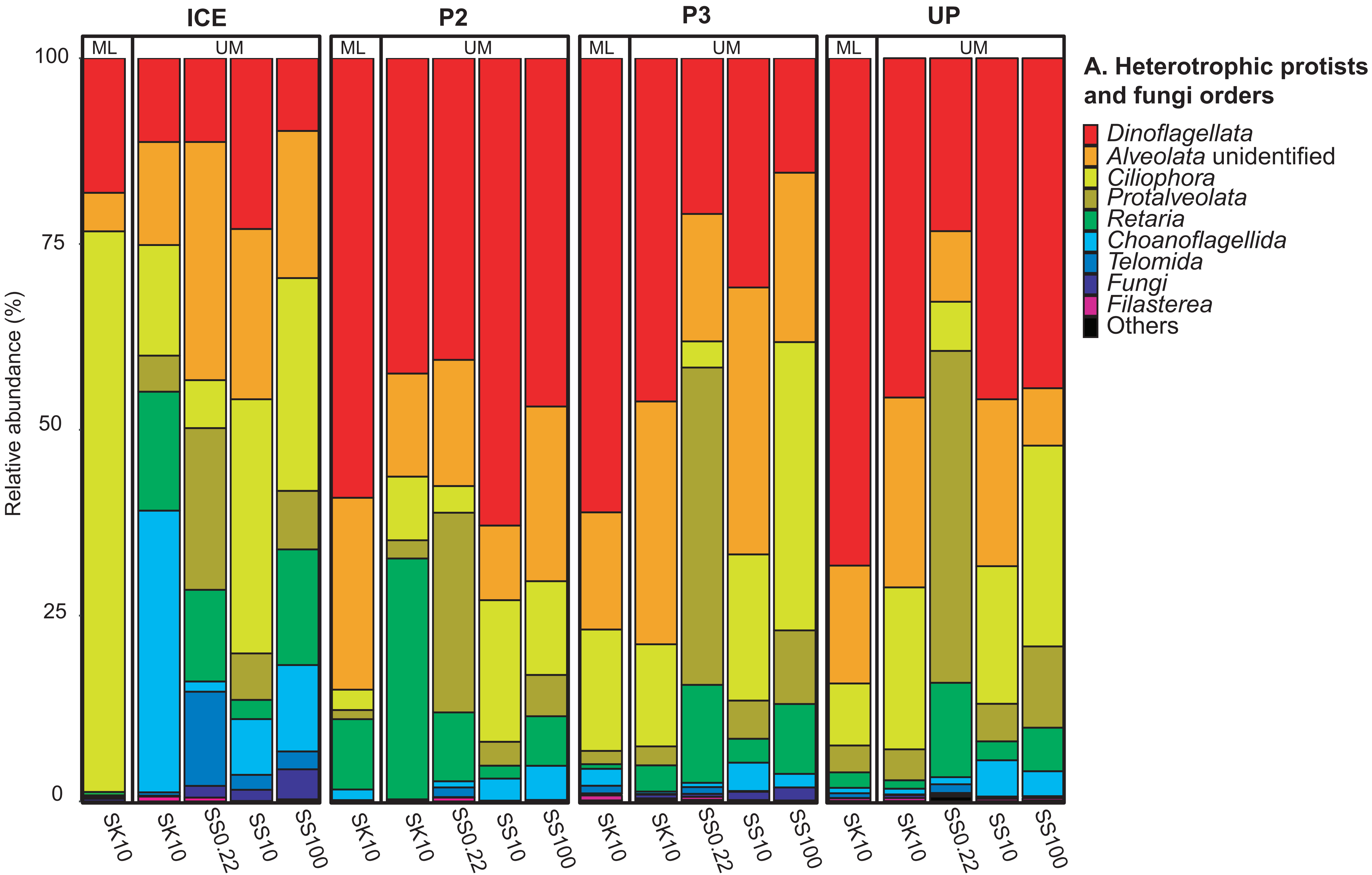


**Fig. S6-A – Taxomomic order composition of heterotrophic protist and fungi communities.** Relative abundance of the 9 most represented taxonomic orders. ML = mixed layer, UM = upper-mesopelagic; SS0.22 = suspended particles 0.22 – 10 μm; SS10 = suspended particles 10 – 100 μm; SS100 = suspended particles ≥ 100 μm; (SS100), SK10 = sinking particles ≥ 10 μm.

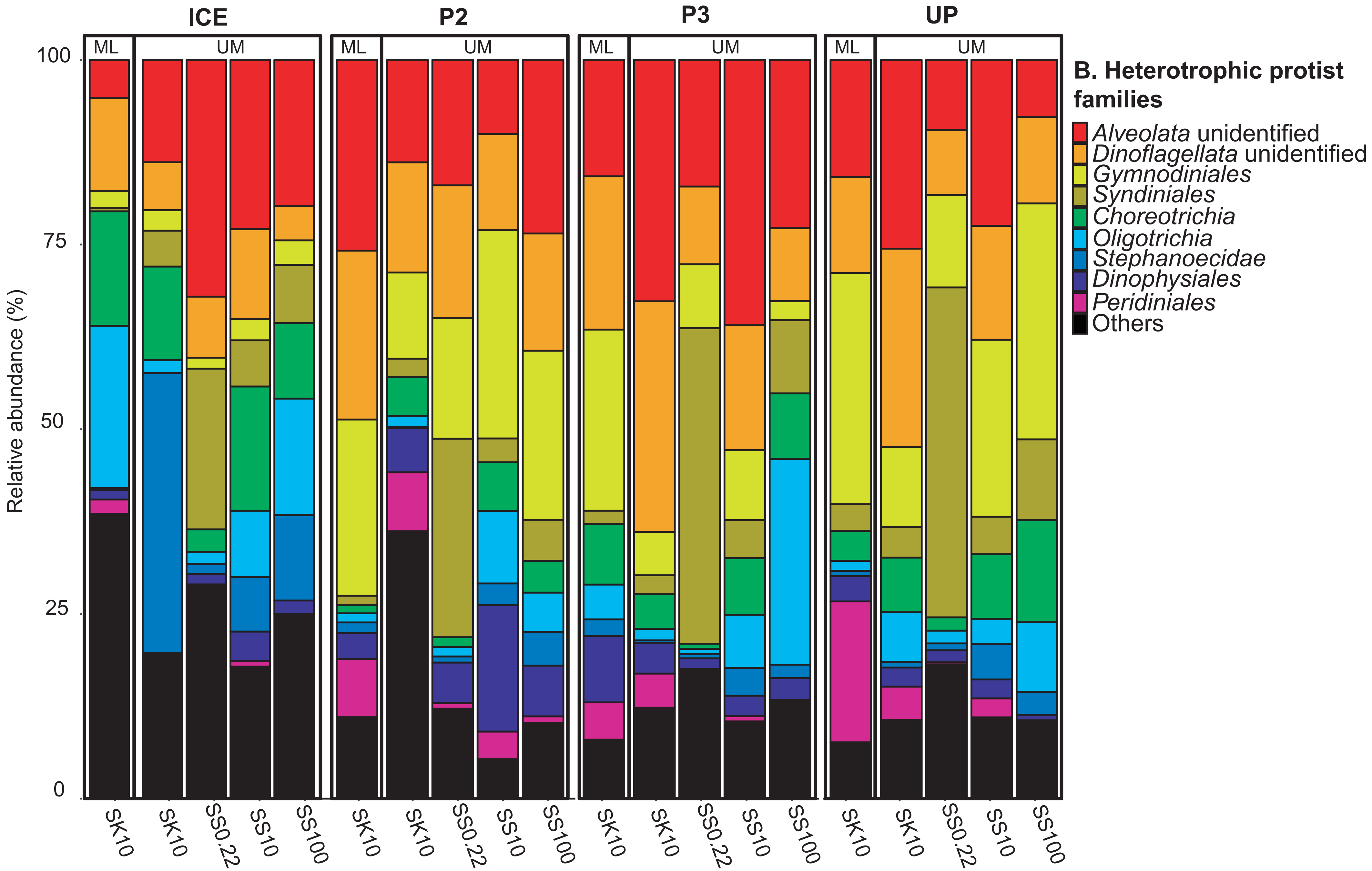


**Fig. S6-B – Taxomomic order composition of heterotrophic protist communities.** Relative abundance of the 9 most represented heterotrophic protist families. ML = mixed layer, UM = upper-mesopelagic; SS0.22 = suspended particles 0.22 – 10 μm; SS10 = suspended particles 10 – 100 μm; SS100 = suspended particles ≥ 100 μm; (SS100), SK10 = sinking particles ≥ 10 μm.

**Table S1 – Sequence counts tables.** Numbers presented in this table are based on PR[2] annotations. The first column displays the number of sequences and the column "%" displays the percentage to the total. Unaffiliated sequences were not reported in this table. ML = mixed layer, UM = upper-mesopelagic; SS0.22 = suspended particles 0.22 – 10 µm; SS10 = suspended particles 10 – 100 µm; SS100 = suspended particles ≥ 100 µm; (SS100), SK10 = sinking particles ≥ 10 µm.

| Station | Depth | Particle type | Total reads | Phytoplankton | % | Metazoa | % | Dinoflagellates | % | Choanoflagellates | % | Ciliates | % | Rhizaria | % | Fungi | % |
|---|---|---|---|---|---|---|---|---|---|---|---|---|---|---|---|---|---|
| ICE | ML | SK10 | 52705 | 522 | 1.0 | 2614 | 5.0 | 11476 | 21.8 | 111 | 0.2 | 37449 | 71.1 | 17 | 0.0 | 172 | 0.3 |
| P2 | ML | SK10 | 64077 | 1561 | 2.4 | 46309 | 72.3 | 13292 | 20.7 | 207 | 0.3 | 412 | 0.6 | 1418 | 2.2 | 4 | 0.0 |
| P3 | ML | SK10 | 40469 | 593 | 1.5 | 29654 | 73.3 | 7755 | 19.2 | 248 | 0.6 | 1633 | 4.0 | 75 | 0.2 | 82 | 0.2 |
| UP | ML | SK10 | 44045 | 517 | 1.2 | 34816 | 79.0 | 7136 | 16.2 | 61 | 0.1 | 711 | 1.6 | 177 | 0.4 | 34 | 0.1 |
| ICE | ML | SS0.22 | 61368 | 28766 | 46.9 | 3 | 0.0 | 18612 | 30.3 | 144 | 0.2 | 4267 | 7.0 | 60 | 0.1 | 786 | 1.3 |
| P2 | ML | SS0.22 | 61107 | 12667 | 20.7 | 3726 | 6.1 | 31226 | 51.1 | 2152 | 3.5 | 6106 | 10.0 | 600 | 1.0 | 41 | 0.1 |
| P3 | ML | SS0.22 | 49647 | 4588 | 9.2 | 1589 | 3.2 | 30832 | 62.1 | 1180 | 2.4 | 4678 | 9.4 | 325 | 0.7 | 799 | 1.6 |
| UP | ML | SS0.22 | 34996 | 2766 | 7.9 | 11358 | 32.5 | 14782 | 42.2 | 826 | 2.4 | 2075 | 5.9 | 100 | 0.3 | 548 | 1.6 |
| ICE | ML | SS10 | 16121 | 1977 | 12.3 | 4 | 0.0 | 6682 | 41.4 | 491 | 3.0 | 5134 | 31.8 | 4 | 0.0 | 55 | 0.3 |
| P2 | ML | SS10 | 38787 | 3791 | 9.8 | 7621 | 19.6 | 18888 | 48.7 | 3626 | 9.3 | 2936 | 7.6 | 344 | 0.9 | 10 | 0.0 |
| P3 | ML | SS10 | 41787 | 3803 | 9.1 | 6587 | 15.8 | 21996 | 52.6 | 1929 | 4.6 | 3301 | 7.9 | 333 | 0.8 | 390 | 0.9 |
| UP | ML | SS10 | 39264 | 4484 | 11.4 | 7731 | 19.7 | 18560 | 47.3 | 2070 | 5.3 | 2206 | 5.6 | 157 | 0.4 | 485 | 1.2 |
| ICE | ML | SS100 | 44855 | 3213 | 7.2 | 227 | 0.5 | 12371 | 27.6 | 1299 | 2.9 | 26494 | 59.1 | 5 | 0.0 | 441 | 1.0 |
| P2 | ML | SS100 | 41798 | 1647 | 3.9 | 26547 | 63.5 | 6680 | 16.0 | 4187 | 10.0 | 2057 | 4.9 | 264 | 0.6 | 11 | 0.0 |
| P3 | ML | SS100 | 25978 | 543 | 2.1 | 18250 | 70.3 | 4738 | 18.2 | 621 | 2.4 | 1379 | 5.3 | 39 | 0.2 | 132 | 0.5 |
| UP | ML | SS100 | 42061 | 1266 | 3.0 | 27851 | 66.2 | 7235 | 17.2 | 1924 | 4.6 | 2650 | 6.3 | 138 | 0.3 | 352 | 0.8 |
| ICE | UM | SK10 | 30666 | 85 | 0.3 | 26240 | 85.6 | 1588 | 5.2 | 78 | 0.3 | 2200 | 7.2 | 51 | 0.2 | 162 | 0.5 |
| P2 | UM | SK10 | 37034 | 179 | 0.5 | 24573 | 66.4 | 6862 | 18.5 | 25 | 0.1 | 1018 | 2.7 | 3972 | 10.7 | 11 | 0.0 |
| P3 | UM | SK10 | 44553 | 241 | 0.5 | 29281 | 65.7 | 11728 | 26.3 | 53 | 0.1 | 2093 | 4.7 | 517 | 1.2 | 118 | 0.3 |
| UP | UM | SK10 | 40694 | 150 | 0.4 | 28874 | 71.0 | 8193 | 20.1 | 92 | 0.2 | 2420 | 5.9 | 134 | 0.3 | 89 | 0.2 |
| ICE | UM | SS0.22 | 55360 | 9636 | 17.4 | 3258 | 5.9 | 17826 | 32.2 | 611 | 1.1 | 2655 | 4.8 | 5317 | 9.6 | 883 | 1.6 |
| P2 | UM | SS0.22 | 40436 | 2117 | 5.2 | 1627 | 4.0 | 20950 | 51.8 | 309 | 0.8 | 1363 | 3.4 | 3350 | 8.3 | 70 | 0.2 |
| P3 | UM | SS0.22 | 45093 | 587 | 1.3 | 4179 | 9.3 | 14841 | 32.9 | 295 | 0.7 | 1554 | 3.4 | 5231 | 11.6 | 419 | 0.9 |
| UP | UM | SS0.22 | 36960 | 546 | 1.5 | 4213 | 11.4 | 10850 | 29.4 | 308 | 0.8 | 2108 | 5.7 | 4019 | 10.9 | 199 | 0.5 |
| ICE | UM | SS10 | 32140 | 545 | 1.7 | 5407 | 16.8 | 11588 | 36.1 | 1929 | 6.0 | 8693 | 27.0 | 676 | 2.1 | 398 | 1.2 |
| P2 | UM | SS10 | 41613 | 518 | 1.2 | 3319 | 8.0 | 27493 | 66.1 | 1100 | 2.6 | 7201 | 17.3 | 689 | 1.7 | 11 | 0.0 |
| P3 | UM | SS10 | 31640 | 225 | 0.7 | 7403 | 23.4 | 16081 | 50.8 | 923 | 2.9 | 4387 | 13.9 | 767 | 2.4 | 288 | 0.9 |
| UP | UM | SS10 | 28927 | 256 | 0.9 | 5819 | 20.1 | 15475 | 53.5 | 1149 | 4.0 | 4153 | 14.4 | 609 | 2.1 | 136 | 0.5 |
| ICE | UM | SS100 | 20787 | 882 | 4.2 | 380 | 1.8 | 5743 | 27.6 | 2326 | 11.2 | 5582 | 26.9 | 3006 | 14.5 | 810 | 3.9 |
| P2 | UM | SS100 | 29117 | 142 | 0.5 | 23278 | 79.9 | 3963 | 13.6 | 259 | 0.9 | 748 | 2.6 | 375 | 1.3 | 8 | 0.0 |
| P3 | UM | SS100 | 6051 | 8 | 0.1 | 2078 | 34.3 | 1215 | 20.1 | 58 | 1.0 | 1234 | 20.4 | 299 | 4.9 | 56 | 0.9 |
| UP | UM | SS100 | 312267 | 1837 | 0.6 | 193112 | 61.8 | 58831 | 18.8 | 3872 | 1.2 | 32055 | 10.3 | 6538 | 2.1 | 506 | 0.2 |

**Table S2 – Station description and particulate organic carbon concentration.** Particulate organic carbon concentrations were measured by and are presented in Belcher et al. (2016). SS = bulk suspended particles; SK = bulk sinking particles.

| Latitude (˚N) | Longitude (˚E) | Station | Station description | Depth (m) | Particle-type | POC (µg $L^{-1}$) |
|---|---|---|---|---|---|---|
| -59.9624 | -46.1597 | ICE | On the Antarctic continental ice edge. | 60 | SS | 75.7 |
| | | | | | SK | 2.5 |
| | | | | 160 | SS | 32.2 |
| | | | | | SK | 10.3 |
| -55.2484 | -41.264 | P2 | HNLC zone. | 55 | SS | 124.6 |
| | | | | | SK | 14.1 |
| | | | | 155 | SS | 38.6 |
| | | | | | SK | 2.7 |
| -52.8121 | -39.9724 | P3 | Iron fertilized zone, near South Georgia continental margin. | 70 | SS | 124.2 |
| | | | | | SK | 5.6 |
| | | | | 170 | SS | 31.4 |
| | | | | | SK | 3.9 |
| -52.6018 | -39.1994 | UP | Upwelling station in proximity to P3, in frontal system PFZ and AAZ. | 70 | SS | 92.2 |
| | | | | | SK | 22.5 |
| | | | | 170 | SS | 45.8 |
| | | | | | SK | 9.1 |

Belcher, A., M. Iversen, C. Manno, S. A. Henson, G. A. Tarling, and R. Sanders. 2016b. The role of particle associated microbes in remineralization of fecal pellets in the upper mesopelagic of the Scotia Sea, Antarctica. Limnol. Oceanogr. 61: 1049–1064. doi:10.1002/lno.10269

**Table S3 – Permutational multivariate analysis of variance of environmental parameters.** Table A displays the PERMANOVA results for phytoplankton community and table B for heterotrophic protist community. Factors highlighted with an asterisk (*) were significantly affecting the OTU composition variability. SS: sums of squares; MS: means of squares; F.Model: F-tests results; R2: effect size; Pr: p-value.

| A - Phytoplankton | | | | | | |
|---|---|---|---|---|---|---|
| | **Df** | **SumsOfSqs** | **MeanSqs** | **F.Model** | **R2** | **Pr(>F)** |
| **Temperature*** | 1 | 0.815 | 0.815 | 4.444 | 17% | 0.001 |
| **Oxygen** | 1 | 0.254 | 0.254 | 1.383 | 5% | 0.137 |
| **Fluorescence*** | 1 | 0.471 | 0.471 | 2.570 | 10% | 0.003 |
| **POC** | 1 | 0.232 | 0.232 | 1.262 | 5% | 0.228 |
| **Type*** | 3 | 0.931 | 0.310 | 1.692 | 19% | 0.014 |
| ***Residuals*** | *12* | *2.202* | *0.183* | *NA* | *45%* | *NA* |
| ***Total*** | *19* | *4.906* | *NA* | *NA* | *1* | *NA* |

| B - Heterotrophic protist and fungi | | | | | | |
|---|---|---|---|---|---|---|
| | **Df** | **SumsOfSqs** | **MeanSqs** | **F.Model** | **R2** | **Pr(>F)** |
| **Temperature*** | 1 | 0.431 | 0.431 | 2.759 | 11% | 0.001 |
| **Oxygen*** | 1 | 0.379 | 0.379 | 2.428 | 9% | 0.002 |
| **Fluorescence*** | 1 | 0.270 | 0.270 | 1.729 | 7% | 0.023 |
| **POC*** | 1 | 0.349 | 0.349 | 2.234 | 9% | 0.004 |
| **Type*** | 3 | 0.752 | 0.251 | 1.604 | 19% | 0.010 |
| ***Residuals*** | *12* | *1.875* | *0.156* | *NA* | *46%* | *NA* |
| ***Total*** | *19* | *4.057* | *NA* | *NA* | *1* | *NA* |

**Table S4 - Taxonomic composition of cyanobacterial sequences.** Table A displays the taxonomic affiliation of cyanobacterial sequebces. Table B displays the number of sequences and table C their relative abundance normalised to the entire 16S rRNA gene amplicon sequencing dataset.

**Table S4-A**

| OTU_ID | Taxonomy |
|---|---|
| AB494937.1.1515 | k__Bacteria; p__Cyanobacteria; c__4C0d-2; o__YS2; f__; g__; s__ |
| AB934802.1.1340 | k__Bacteria; p__Cyanobacteria; c__4C0d-2; o__YS2; f__; g__; s__ |
| KP765487.1.1505 | k__Bacteria; p__Cyanobacteria; c__4C0d-2; o__YS2; f__; g__; s__ |
| New.CleanUp.ReferenceOTU108 | k__Bacteria; p__Cyanobacteria; c__4C0d-2; o__YS2; f__; g__; s__ |
| New.CleanUp.ReferenceOTU649 | k__Bacteria; p__Cyanobacteria; c__4C0d-2; o__YS2; f__; g__; s__ |
| JQ855618.1.1256 | k__Bacteria; p__Cyanobacteria; c__Nostocophycideae; o__Nostocales; f__Nostocaceae |
| BA000022.2452187.2453675 | k__Bacteria; p__Cyanobacteria; c__Oscillatoriophycideae; o__Chroococcales; f__Gomphosphaeriaceae; g__; s__ |
| GU935367.1.1704 | k__Bacteria; p__Cyanobacteria; c__Oscillatoriophycideae; o__Chroococcales; f__Gomphosphaeriaceae; g__; s__ |
| CP003597.5559716.5561195 | k__Bacteria; p__Cyanobacteria; c__Oscillatoriophycideae; o__Chroococcales; f__Xenococcaceae; g__; s__ |
| JF199033.1.1311 | k__Bacteria; p__Cyanobacteria; c__Oscillatoriophycideae; o__Chroococcales; f__Xenococcaceae; g__; s__ |
| CP000393.3137164.3138645 | k__Bacteria; p__Cyanobacteria; c__Oscillatoriophycideae; o__Oscillatoriales; f__Phormidiaceae; g__Hydrocoleum |
| KM982579.1.1437 | k__Bacteria; p__Cyanobacteria; c__Oscillatoriophycideae; o__Oscillatoriales; f__Phormidiaceae; g__Hydrocoleum; s__ |
| HQ189027.1.1331 | k__Bacteria; p__Cyanobacteria; c__Oscillatoriophycideae; o__Oscillatoriales; f__Phormidiaceae; g__Phormidium; s__ |
| New.CleanUp.ReferenceOTU718 | k__Bacteria; p__Cyanobacteria; c__Synechococcophycideae; o__Pseudanabaenales; f__Pseudanabaenaceae; g__Leptolyngbya; s__ |
| EF032663.1.1445 | k__Bacteria; p__Cyanobacteria; c__Synechococcophycideae; o__Synechococcales; f__Chamaesiphonaceae; g__; s__ |
| FJ937850.1.1317 | k__Bacteria; p__Cyanobacteria; c__Synechococcophycideae; o__Synechococcales; f__Synechococcaceae; g__Synechococcus; s__ |
| FR667282.1.1373 | k__Bacteria; p__Cyanobacteria; c__Synechococcophycideae; o__Synechococcales; f__Synechococcaceae; g__Synechococcus; s__ |
| GU305749.1.1449 | k__Bacteria; p__Cyanobacteria; c__Synechococcophycideae; o__Synechococcales; f__Synechococcaceae; g__Synechococcus; s__ |
| GU941055.1.1253 | k__Bacteria; p__Cyanobacteria; c__Synechococcophycideae; o__Synechococcales; f__Synechococcaceae; g__Synechococcus; s__ |
| HQ671782.1.1436 | k__Bacteria; p__Cyanobacteria; c__Synechococcophycideae; o__Synechococcales; f__Synechococcaceae; g__Synechococcus; s__ |
| JQ062791.1.1291 | k__Bacteria; p__Cyanobacteria; c__Synechococcophycideae; o__Synechococcales; f__Synechococcaceae; g__Synechococcus; s__ |

**Table S4-B**

| OTU_ID | ICE_SK10_UM | ICE_SK10_ML | ICE_SS0.22_UI | ICE_SS0.22_MI | ICE_SS10_UM | ICE_SS10_ML | ICE_SS100_UI | ICE_SS100_ML | P2_SK10_UM | P2_SK10_ML | P2_SS0.22_UM | P2_SS0.22_ML | P2_SS10_UM | P2_SS10_ML | P2_SS100_UM | P2_SS100_ML |
|---|---|---|---|---|---|---|---|---|---|---|---|---|---|---|---|---|
| AB494937.1.1515 | 0 | 0 | 0 | 0 | 0 | 0 | 0 | 2 | 0 | 0 | 0 | 0 | 0 | 0 | 0 | 0 |
| AB934802.1.1340 | 0 | 0 | 0 | 0 | 0 | 0 | 0 | 4 | 0 | 0 | 0 | 0 | 0 | 0 | 0 | 0 |
| KP765487.1.1505 | 0 | 0 | 0 | 0 | 0 | 0 | 0 | 2 | 0 | 0 | 0 | 0 | 0 | 0 | 0 | 0 |
| New.CleanUp.ReferenceOTU108 | 0 | 0 | 0 | 0 | 0 | 0 | 0 | 3 | 0 | 0 | 0 | 0 | 0 | 0 | 0 | 0 |
| New.CleanUp.ReferenceOTU649 | 0 | 0 | 0 | 0 | 0 | 0 | 0 | 2 | 0 | 0 | 0 | 0 | 0 | 0 | 0 | 0 |
| JQ855618.1.1256 | 0 | 0 | 0 | 0 | 0 | 0 | 0 | 0 | 0 | 0 | 0 | 0 | 0 | 0 | 0 | 0 |
| BA000022.2452187.2453675 | 0 | 0 | 0 | 0 | 0 | 1 | 0 | 0 | 0 | 0 | 0 | 0 | 0 | 0 | 0 | 0 |
| GU935367.1.1704 | 0 | 0 | 0 | 0 | 0 | 0 | 1 | 0 | 0 | 0 | 0 | 0 | 0 | 0 | 0 | 0 |
| CP003597.5559716.5561195 | 0 | 0 | 0 | 0 | 0 | 0 | 0 | 0 | 0 | 0 | 0 | 0 | 0 | 0 | 0 | 0 |
| JF199033.1.1311 | 0 | 0 | 0 | 0 | 0 | 0 | 0 | 0 | 0 | 0 | 0 | 0 | 0 | 0 | 0 | 0 |
| CP000393.3137164.3138645 | 0 | 0 | 0 | 0 | 0 | 0 | 0 | 0 | 0 | 0 | 0 | 0 | 0 | 2 | 0 | 0 |
| KM982579.1.1437 | 0 | 0 | 0 | 1 | 0 | 0 | 0 | 1 | 0 | 0 | 0 | 1 | 0 | 1 | 0 | 0 |
| HQ189027.1.1331 | 0 | 0 | 0 | 0 | 0 | 0 | 0 | 0 | 0 | 0 | 0 | 0 | 0 | 0 | 0 | 0 |
| New.CleanUp.ReferenceOTU718 | 0 | 0 | 0 | 0 | 0 | 0 | 0 | 0 | 0 | 0 | 0 | 0 | 0 | 0 | 0 | 0 |
| EF032663.1.1445 | 0 | 0 | 0 | 0 | 0 | 0 | 0 | 0 | 0 | 0 | 0 | 0 | 0 | 0 | 0 | 0 |
| FJ937850.1.1317 | 3 | 0 | 0 | 0 | 0 | 0 | 0 | 0 | 0 | 0 | 0 | 0 | 0 | 0 | 0 | 0 |
| FR667282.1.1373 | 0 | 0 | 0 | 0 | 0 | 0 | 0 | 0 | 0 | 0 | 0 | 0 | 1 | 0 | 0 | 0 |
| GU305749.1.1449 | 0 | 0 | 0 | 0 | 0 | 0 | 0 | 0 | 0 | 0 | 0 | 0 | 0 | 0 | 3 | 0 |
| GU941055.1.1253 | 5 | 0 | 0 | 0 | 1 | 0 | 0 | 0 | 0 | 0 | 0 | 0 | 0 | 0 | 0 | 0 |
| HQ671782.1.1436 | 0 | 0 | 0 | 0 | 0 | 0 | 0 | 0 | 0 | 0 | 0 | 0 | 0 | 0 | 0 | 0 |
| JQ062791.1.1291 | 0 | 0 | 0 | 0 | 0 | 0 | 0 | 12 | 0 | 0 | 0 | 0 | 0 | 0 | 0 | 0 |
| **Total** | **8** | **0** | **0** | **1** | **1** | **1** | **1** | **26** | **0** | **0** | **0** | **1** | **1** | **3** | **3** | **0** |

| OTU_ID | P3_SK10_UM | P3_SK10_ML | P3_SS0.22_UM | P3_SS0.22_ML | P3_SS10_UM | P3_SS10_ML | P3_SS100_UM | P3_SS100_ML | UP_SK10_UM | UP_SK10_ML | UP_SS0.22_UI | UP_SS0.22_ML | UP_SS10_UM | UP_SS10_ML | UP_SS100_UM | UP_SS100_ML |
|---|---|---|---|---|---|---|---|---|---|---|---|---|---|---|---|---|
| AB494937.1.1515 | 0 | 0 | 0 | 0 | 0 | 0 | 0 | 0 | 0 | 0 | 0 | 0 | 0 | 0 | 0 | 0 |
| AB934802.1.1340 | 0 | 0 | 0 | 0 | 0 | 0 | 0 | 0 | 0 | 0 | 0 | 0 | 0 | 0 | 0 | 0 |
| KP765487.1.1505 | 0 | 0 | 0 | 0 | 0 | 0 | 0 | 0 | 0 | 0 | 0 | 0 | 0 | 0 | 0 | 0 |
| New.CleanUp.ReferenceOTU108 | 0 | 0 | 0 | 0 | 0 | 0 | 0 | 0 | 0 | 0 | 0 | 0 | 0 | 0 | 0 | 0 |
| New.CleanUp.ReferenceOTU649 | 0 | 0 | 0 | 0 | 0 | 0 | 0 | 0 | 0 | 0 | 0 | 0 | 0 | 0 | 0 | 0 |
| JQ855618.1.1256 | 0 | 0 | 0 | 0 | 0 | 0 | 2 | 0 | 0 | 0 | 0 | 0 | 0 | 0 | 0 | 0 |
| BA000022.2452187.2453675 | 0 | 0 | 0 | 0 | 0 | 0 | 0 | 0 | 0 | 0 | 1 | 0 | 0 | 0 | 0 | 0 |
| GU935367.1.1704 | 0 | 0 | 1 | 0 | 0 | 0 | 0 | 0 | 0 | 0 | 1 | 0 | 0 | 0 | 1 | 0 |
| CP003597.5559716.5561195 | 0 | 0 | 0 | 0 | 0 | 0 | 0 | 0 | 2 | 0 | 0 | 0 | 0 | 0 | 0 | 0 |
| JF199033.1.1311 | 0 | 0 | 0 | 0 | 0 | 0 | 27 | 0 | 0 | 0 | 0 | 0 | 0 | 0 | 0 | 0 |
| CP000393.3137164.3138645 | 0 | 0 | 0 | 0 | 0 | 1 | 0 | 0 | 0 | 0 | 0 | 0 | 0 | 0 | 0 | 0 |
| KM982579.1.1437 | 1 | 0 | 0 | 1 | 0 | 3 | 0 | 0 | 0 | 0 | 0 | 0 | 0 | 0 | 1 | 0 |
| HQ189027.1.1331 | 5 | 0 | 0 | 0 | 0 | 0 | 0 | 0 | 0 | 0 | 0 | 0 | 0 | 0 | 0 | 0 |
| New.CleanUp.ReferenceOTU718 | 3 | 0 | 0 | 0 | 0 | 0 | 0 | 0 | 0 | 0 | 0 | 0 | 0 | 0 | 0 | 0 |
| EF032663.1.1445 | 0 | 1 | 0 | 0 | 0 | 0 | 0 | 0 | 1 | 0 | 0 | 0 | 0 | 0 | 0 | 0 |
| FJ937850.1.1317 | 3 | 0 | 0 | 0 | 0 | 0 | 0 | 0 | 0 | 0 | 0 | 0 | 0 | 0 | 0 | 0 |
| FR667282.1.1373 | 0 | 0 | 0 | 0 | 0 | 0 | 0 | 0 | 0 | 0 | 0 | 0 | 0 | 0 | 0 | 0 |
| GU305749.1.1449 | 0 | 0 | 0 | 0 | 0 | 0 | 0 | 0 | 0 | 0 | 0 | 0 | 0 | 0 | 0 | 0 |
| GU941055.1.1253 | 0 | 0 | 0 | 0 | 0 | 0 | 0 | 0 | 0 | 0 | 0 | 0 | 0 | 0 | 0 | 0 |
| HQ671782.1.1436 | 0 | 0 | 1 | 0 | 0 | 0 | 0 | 0 | 0 | 0 | 0 | 0 | 0 | 0 | 4 | 0 |
| JQ062791.1.1291 | 0 | 0 | 0 | 0 | 0 | 0 | 0 | 0 | 0 | 0 | 0 | 0 | 0 | 0 | 0 | 0 |
| **Total** | **12** | **1** | **2** | **1** | **0** | **4** | **29** | **0** | **3** | **0** | **2** | **0** | **0** | **0** | **6** | **0** |

## Table S4-C

| OTU_ID | ICE_SK10_UM | ICE_SK10_ML | ICE_SS0.22_UI | ICE_SS0.22_MI | ICE_SS10_UM | ICE_SS10_ML | ICE_SS100_UI | ICE_SS100_ML | P2_SK10_UM | P2_SK10_ML | P2_SS0.22_UM | P2_SS0.22_ML | P2_SS10_UM | P2_SS10_ML | P2_SS100_UM | P2_SS100_ML |
|---|---|---|---|---|---|---|---|---|---|---|---|---|---|---|---|---|
| AB934802.1.1340 | 0 | 0 | 0 | 0 | 0 | 0 | 0 | 0.006% | 0 | 0 | 0 | 0 | 0 | 0 | 0 | 0 |
| AB494937.1.1515 | 0 | 0 | 0 | 0 | 0 | 0 | 0 | 0.003% | 0 | 0 | 0 | 0 | 0 | 0 | 0 | 0 |
| KP765487.1.1505 | 0 | 0 | 0 | 0 | 0 | 0 | 0 | 0.003% | 0 | 0 | 0 | 0 | 0 | 0 | 0 | 0 |
| New.CleanUp.ReferenceOTU649 | 0 | 0 | 0 | 0 | 0 | 0 | 0 | 0.003% | 0 | 0 | 0 | 0 | 0 | 0 | 0 | 0 |
| New.CleanUp.ReferenceOTU108 | 0 | 0 | 0 | 0 | 0 | 0 | 0 | 0.005% | 0 | 0 | 0 | 0 | 0 | 0 | 0 | 0 |
| JQ855618.1.1256 | 0 | 0 | 0 | 0 | 0 | 0 | 0 | 0 | 0 | 0 | 0 | 0 | 0 | 0 | 0 | 0 |
| BA000022.2452187.2453675 | 0 | 0 | 0 | 0 | 0 | 0.030% | 0 | 0 | 0 | 0 | 0 | 0 | 0 | 0 | 0 | 0 |
| GU935367.1.1704 | 0 | 0 | 0 | 0 | 0 | 0 | 0.019% | 0 | 0 | 0 | 0 | 0 | 0 | 0 | 0 | 0 |
| CP003597.5559716.5561195 | 0 | 0 | 0 | 0 | 0 | 0 | 0 | 0 | 0 | 0 | 0 | 0 | 0 | 0 | 0 | 0 |
| JF199033.1.1311 | 0 | 0 | 0 | 0 | 0 | 0 | 0 | 0 | 0 | 0 | 0 | 0 | 0 | 0 | 0 | 0 |
| CP000393.3137164.3138645 | 0 | 0 | 0 | 0 | 0 | 0 | 0 | 0 | 0 | 0 | 0 | 0 | 0 | 0.038% | 0 | 0 |
| KM982579.1.1437 | 0 | 0 | 0 | 0.015% | 0 | 0 | 0 | 0.002% | 0 | 0 | 0 | 0.009% | 0 | 0.019% | 0 | 0 |
| HQ189027.1.1331 | 0 | 0 | 0 | 0 | 0 | 0 | 0 | 0 | 0 | 0 | 0 | 0 | 0 | 0 | 0 | 0 |
| New.CleanUp.ReferenceOTU718 | 0 | 0 | 0 | 0 | 0 | 0 | 0 | 0 | 0 | 0 | 0 | 0 | 0 | 0 | 0 | 0 |
| EF032663.1.1445 | 0 | 0 | 0 | 0 | 0 | 0 | 0 | 0 | 0 | 0 | 0 | 0 | 0 | 0 | 0 | 0 |
| FR667282.1.1373 | 0 | 0 | 0 | 0 | 0 | 0 | 0 | 0 | 0 | 0 | 0 | 0 | 0.007% | 0 | 0 | 0 |
| GU305749.1.1449 | 0 | 0 | 0 | 0 | 0 | 0 | 0 | 0 | 0 | 0 | 0 | 0 | 0 | 0 | 0.036% | 0 |
| FJ937850.1.1317 | 0.071% | 0 | 0 | 0 | 0 | 0 | 0 | 0 | 0 | 0 | 0 | 0 | 0 | 0 | 0 | 0 |
| HQ671782.1.1436 | 0 | 0 | 0 | 0 | 0 | 0 | 0 | 0 | 0 | 0 | 0 | 0 | 0 | 0 | 0 | 0 |
| GU941055.1.1253 | 0.119% | 0 | 0 | 0 | 0.016% | 0 | 0 | 0 | 0 | 0 | 0 | 0 | 0 | 0 | 0 | 0 |
| JQ062791.1.1291 | 0 | 0 | 0 | 0 | 0 | 0 | 0 | 0.019% | 0 | 0 | 0 | 0 | 0 | 0 | 0 | 0 |
| **Total** | **0.190%** | **0** | **0** | **0.015%** | **0.016%** | **0.030%** | **0.019%** | **0.042%** | **0** | **0** | **0** | **0.009%** | **0.007%** | **0.058%** | **0.036%** | **0** |

| OTU_ID | P3_SK10_UM | P3_SK10_ML | P3_SS0.22_UM | P3_SS0.22_ML | P3_SS10_UM | P3_SS10_ML | P3_SS100_UM | P3_SS100_ML | UP_SK10_UM | UP_SK10_ML | UP_SS0.22_UI | UP_SS0.22_ML | UP_SS10_UM | UP_SS10_ML | UP_SS100_UM | UP_SS100_ML |
|---|---|---|---|---|---|---|---|---|---|---|---|---|---|---|---|---|
| AB934802.1.1340 | 0 | 0 | 0 | 0 | 0 | 0 | 0 | 0 | 0 | 0 | 0 | 0 | 0 | 0 | 0 | 0 |
| AB494937.1.1515 | 0 | 0 | 0 | 0 | 0 | 0 | 0 | 0 | 0 | 0 | 0 | 0 | 0 | 0 | 0 | 0 |
| KP765487.1.1505 | 0 | 0 | 0 | 0 | 0 | 0 | 0 | 0 | 0 | 0 | 0 | 0 | 0 | 0 | 0 | 0 |
| New.CleanUp.ReferenceOTU649 | 0 | 0 | 0 | 0 | 0 | 0 | 0 | 0 | 0 | 0 | 0 | 0 | 0 | 0 | 0 | 0 |
| New.CleanUp.ReferenceOTU108 | 0 | 0 | 0 | 0 | 0 | 0 | 0 | 0 | 0 | 0 | 0 | 0 | 0 | 0 | 0 | 0 |
| JQ855618.1.1256 | 0 | 0 | 0 | 0 | 0 | 0 | 0.004% | 0 | 0 | 0 | 0 | 0 | 0 | 0 | 0 | 0 |
| BA000022.2452187.2453675 | 0 | 0 | 0 | 0 | 0 | 0 | 0 | 0 | 0 | 0 | 0.007% | 0 | 0 | 0 | 0 | 0 |
| GU935367.1.1704 | 0 | 0 | 0.003% | 0 | 0 | 0 | 0 | 0 | 0 | 0 | 0.007% | 0 | 0 | 0 | 0.002% | 0 |
| CP003597.5559716.5561195 | 0 | 0 | 0 | 0 | 0 | 0 | 0 | 0 | 0.016% | 0 | 0 | 0 | 0 | 0 | 0 | 0 |
| JF199033.1.1311 | 0 | 0 | 0 | 0 | 0 | 0 | 0.049% | 0 | 0 | 0 | 0 | 0 | 0 | 0 | 0 | 0 |
| CP000393.3137164.3138645 | 0 | 0 | 0 | 0 | 0 | 0.000% | 0 | 0 | 0 | 0 | 0 | 0 | 0 | 0 | 0 | 0 |
| KM982579.1.1437 | 0.013% | 0 | 0 | 0.006% | 0 | 0.001% | 0 | 0 | 0 | 0 | 0 | 0 | 0 | 0 | 0.002% | 0 |
| HQ189027.1.1331 | 0.065% | 0 | 0 | 0 | 0 | 0 | 0 | 0 | 0 | 0 | 0 | 0 | 0 | 0 | 0 | 0 |
| New.CleanUp.ReferenceOTU718 | 0.039% | 0 | 0 | 0 | 0 | 0 | 0 | 0 | 0 | 0 | 0 | 0 | 0 | 0 | 0 | 0 |
| EF032663.1.1445 | 0 | 0.012% | 0 | 0 | 0 | 0 | 0 | 0 | 0.008% | 0 | 0 | 0 | 0 | 0 | 0 | 0 |
| FR667282.1.1373 | 0 | 0 | 0 | 0 | 0 | 0 | 0 | 0 | 0 | 0 | 0 | 0 | 0 | 0 | 0 | 0 |
| GU305749.1.1449 | 0 | 0 | 0 | 0 | 0 | 0 | 0 | 0 | 0 | 0 | 0 | 0 | 0 | 0 | 0 | 0 |
| FJ937850.1.1317 | 0.039% | 0 | 0 | 0 | 0 | 0 | 0 | 0 | 0 | 0 | 0 | 0 | 0 | 0 | 0 | 0 |
| HQ671782.1.1436 | 0 | 0 | 0.003% | 0 | 0 | 0 | 0 | 0 | 0 | 0 | 0 | 0 | 0 | 0 | 0.010% | 0 |
| GU941055.1.1253 | 0 | 0 | 0 | 0 | 0 | 0 | 0 | 0 | 0 | 0 | 0 | 0 | 0 | 0 | 0 | 0 |
| JQ062791.1.1291 | 0 | 0 | 0 | 0 | 0 | 0 | 0 | 0 | 0 | 0 | 0 | 0 | 0 | 0 | 0 | 0 |
| **Total** | **0.157%** | **0.012%** | **0.005%** | **0.006%** | **0** | **0.001%** | **0.052%** | **0** | **0.024%** | **0** | **0.014%** | **0** | **0** | **0** | **0.014%** | **0** |

**Table S5 - Dissimilarity values from similarity percentages analyses of heterotrophic protist community.** Dissimilarity between particle-types in the upper-mesopelagic were calculated on rarefied dataset based on results from a SIMPER analyses.

**ICE**

| | SK10 | SS100 | SS10 | SS0.22 |
|---|---|---|---|---|
| **SK10** | | 95.7% | 89.3% | 88.9% |
| **SS100** | | | 44.0% | 53.5% |
| **SS10** | | | | 54.8% |
| **SS0.22** | | | | |

**P2**

| | SK10 | SS100 | SS10 | SS0.22 |
|---|---|---|---|---|
| **SK10** | | 52.2% | 57.1% | 63.4% |
| **SS100** | | | 37.5% | 49.9% |
| **SS10** | | | | 56.2% |
| **SS0.22** | | | | |

**P3**

| | SK10 | SS100 | SS10 | SS0.22 |
|---|---|---|---|---|
| **SK10** | | 62.9% | 43.5% | 62.6% |
| **SS100** | | | 52.7% | 64.5% |
| **SS10** | | | | 57.5% |
| **SS0.22** | | | | |

**UP**

| | SK10 | SS100 | SS10 | SS0.22 |
|---|---|---|---|---|
| **SK10** | | 56.6% | 34.9% | 63.3% |
| **SS100** | | | 41.5% | 62.3% |
| **SS10** | | | | 59.8% |
| **SS0.22** | | | | |